Jamming of Wireless Localization Systems

Sinan Gezici, *Senior Member, IEEE*, Mohammad Reza Gholami, *Member, IEEE*, Suat Bayram *Member, IEEE*, and Magnus Jansson

***Abstract*— In this paper, the optimal jamming of wireless localization systems is investigated. Two optimal power allocation schemes are proposed for jammer nodes in the presence of total and peak power constraints. In the first scheme, power is allocated to jammer nodes in order to maximize the average Cramér–Rao lower bound (CRLB) of target nodes, whereas in the second scheme, the power allocation is performed for the aim of maximizing the minimum CRLB of target nodes. Both the schemes are formulated as linear programs, and a closed-form solution is obtained for the first scheme. For the second scheme, under certain conditions, the property of full total power utilization is specified, and a closed-form solution is obtained when the total power is lower than a specific threshold. In addition, it is shown that non-zero power is allocated to at most N_T jammer nodes according to the second scheme in the absence of peak power constraints, where N_T is the number of target nodes. In the presence of parameter uncertainty, robust versions of the power allocation schemes are proposed. Simulation results are presented to investigate the performance of the proposed schemes and to illustrate the theoretical results.**

***Index Terms*— Localization, jammer, power allocation, Cramér-Rao lower bound.**

I. Introduction

OVER the last two decades, wireless localization has not only become an important application for various systems and services, but also drawn significant interest from research communities [2]–[4]. Among various applications of wireless localization are inventory tracking, home automation, tracking of robots, fire-fighters and miners, patient monitoring, and intelligent transport systems [5]. In order to realize such applications under certain accuracy requirements, both theoretical and experimental studies have been performed in the literature (e.g., [6] and [7]).

Even though various studies have been conducted on wireless localization, jamming of wireless *localization* systems has not been investigated thoroughly. In the literature, there exist some studies on GPS jamming and anti-jamming, such as [8]–[10]. However, for a given wireless localization system, a general theoretical analysis that quantifies the effects of multiple jammer nodes on localization accuracy has not been performed, and optimal jamming strategies have not been investigated before to the best of authors' knowledge (see [1] for the conference version of this study).

Although there exists no previous work on optimal power allocation for jammer nodes in a wireless localization system, power allocation for wireless localization and radar systems has recently been considered in [11]–[20]. The study in [11] considers the minimization of the squared position error bound (SPEB) for the purpose of optimal anchor power allocation, anchor selection, or anchor deployment. In [14], optimal transmit power allocation is performed for anchor nodes in order to minimize the SPEB and the maximum directional position error bound (mDPEB) of the wireless localization system. Conic programming is employed for efficient solutions, and improvements over uniform power allocation are illustrated. In the presence of parameter uncertainty, the studies in [13] and [14] provide robust power allocation strategies for wireless localization systems. In [15], ranging energy optimization is studied for a wireless localization system that employs two-way ranging between a target node and anchor nodes by considering a specific accuracy requirement in a prescribed service area. In addition to the formulation of ranging energy optimization problems, a practical algorithm is proposed based on semidefinite programming. The problem in [15] is investigated in the presence of collaborative nodes in [16], and the corresponding ranging energy optimization problem and a practical algorithm is proposed. In [17], the optimal power allocation strategies are investigated for target localization in a distributed multiple-radar system, where the total transmit power and the Cramér-Rao lower bound (CRLB) are considered as the two metrics in the optimization problems. Due to non-convexity of the optimization problems, relaxation and domain decomposition methods are employed, which facilitate both central processing at the fusion center and distributed processing.

The studies in [19] and [20] consider the optimal power allocation problem for both wireless network localization (active) and multiple radar localization (passive) systems. Based on the convexity and lower rank properties of the SPEB, the power allocation problems are transformed into second-order cone programs (SOCPs), leading to efficient solutions. In addition, in the presence of parameter uncertainty, robust power allocation algorithms are developed. In [21] and [22], joint power and bandwidth allocation is studied for wireless

Manuscript received August 10, 2015; revised January 4, 2016 and February 29, 2016; accepted April 22, 2016. Date of publication April 23, 2016; date of current version June 14, 2016. This work was supported in part by the Distinguished Young Scientist Award of Turkish Academy of Sciences (TUBA-GEBIP 2013). This work was presented at the IEEE International Conference on Communications Workshops 2015, London, U.K., June 2015 [1]. The associate editor coordinating the review of this paper and approving it for publication was G. Abreu.

S. Gezici is with the Department of Electrical and Electronics Engineering, Bilkent University, Ankara 06800, Turkey (e-mail: gezici@ee.bilkent.edu.tr).

M. R. Gholami is with Campanja AB, Stockholm SE-111 57, Sweden (e-mail: mohrg@kth.se).

S. Bayram is with the Department of Electrical and Electronics Engineering, Turgut Ozal University, Ankara 06010, Turkey (e-mail: sbayram@turgutozal.edu.tr).

M. Jansson is with the ACCESS Linnaeus Centre, Electrical Engineering, KTH Royal Institute of Technology, Stockholm 100 44, Sweden (e-mail: janssonm@kth.se).

Color versions of one or more of the figures in this paper are available online at http://ieeexplore.ieee.org.

Digital Object Identifier 10.1109/TCOMM.2016.2558560

localization systems. In particular, the optimal power and bandwidth allocation problem is formulated for cooperative localization systems in [21], and the resulting non-convex problem is solved approximately based on Taylor expansion, and iterative optimization of power and bandwidth separately. In [22], robust power and bandwidth allocation problems are proposed for wireless localization systems in order to optimize localization accuracy or energy consumption in the presence of uncertainty about positions of target nodes. In [23]–[26], the problem of jammer localization is studied, where the aim is to determine positions of jammer nodes in the system, which is a different problem from the optimal jamming of wireless localization systems considered in this manuscript. In a recent study [27], the optimal placement of a single jammer node with a fixed power is investigated for degrading the localization accuracy of a wireless network based on the problem formulation in [1]. Due to the non-convexity of the optimal placement problem, the solution is provided only for special scenarios [27].

Unlike the power allocation studies for wireless localization and radar systems in the literature [11]–[20], this study investigates the optimal power allocation problem for jammer nodes in order to degrade the performance of a given wireless localization system. In particular, the optimal power allocation is performed for jammer nodes to maximize either the average CRLB or the minimum CRLB of the target nodes. There are two main motivations behind this study: (i) To provide guidelines for developing jamming schemes for disabling a wireless localization system (e.g., of an enemy). (ii) To obtain theoretical results that are useful for developing anti-jamming systems. The main contributions of this study can be summarized as follows:

- Optimal power allocation strategies are investigated for jammer nodes in a wireless localization system for the first time.
- Two optimal power allocation schemes are developed for jammer nodes to maximize the average or the minimum of the CRLBs for target nodes. Both schemes are formulated as linear programs.
- A closed-form solution is obtained for the scheme that maximizes the average CRLB.
- For the scheme that maximizes the minimum CRLB, a closed-form solution is obtained when the total power limit is lower than a specific threshold.
- In the absence of peak power constraints, it is proved that non-zero power is allocated to at most N_T jammer nodes for maximizing the minimum CRLB, where N_T is the number of target nodes.
- The proposed jamming strategies are extended to scenarios with parameter uncertainty to provide robust jamming performance.

The remainder of the manuscript is organized as follows. In Section II, the system model is introduced. In Section III, two power allocation formulations are proposed for optimal jamming of wireless localization systems, and the optimal power allocation schemes are characterized via theoretical analyses. Robust versions of the proposed jamming strategies are developed in Section IV. Simulation results are presented in Section V, and concluding remarks are made in Section VII.

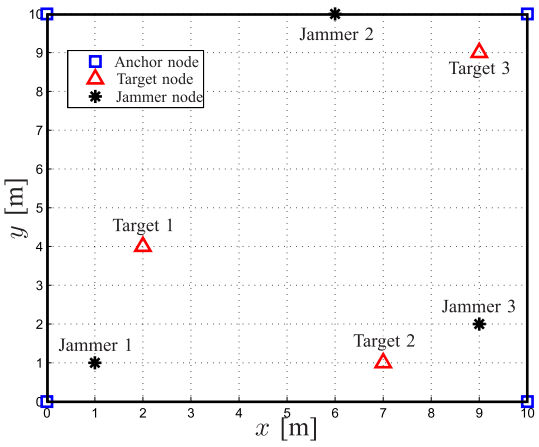

Fig. 1. The network considered in the simulations, where the anchor node positions are [0 0], [10 0], [0 10], and [10 10] m., the target node positions are [2 4], [7 1], and [9 9] m., and the jammer node positions are [1 1], [6 10], and [9 2] m.

II. System Model

Consider a wireless localization system consisting of N_A anchor nodes and N_T target nodes located at $\boldsymbol{y}_i \in \mathbb{R}^2$, $i = 1, \ldots, N_A$ and $\boldsymbol{x}_i \in \mathbb{R}^2$, $i = 1, \ldots, N_T$, respectively.[1] It is assumed that the target nodes estimate their locations based on received signals from the anchor nodes, which have known locations; that is, self-positioning is considered [5]. In addition to the target and anchor nodes, there exist N_J jammer nodes at $\boldsymbol{z}_i \in \mathbb{R}^2$, $i = 1, \ldots, N_J$ in the system, which aim to degrade the localization performance of the system. The jammer nodes are modeled to transmit Gaussian noise[2] in accordance with the common approach in the literature [28]–[30]. An example of the proposed system model is shown in Fig. 1, where there are four anchor nodes ($N_A = 4$), three target nodes ($N_T = 3$), and three jammer nodes ($N_J = 3$).

In this study, non-cooperative localization is considered; that is, target nodes are assumed to receive signals only from anchor nodes (i.e., not from other target nodes) for localization purposes. In addition, the connectivity sets are defined as $\mathcal{A}_i \triangleq \{j \in \{1, \ldots, N_A\} |$ anchor node j is connected to target node $i\}$ for $i \in \{1, \ldots, N_T\}$. Then, the received signal at target node i coming from anchor node j can be expressed as

$$r_{ij}(t) = \sum_{k=1}^{L_{ij}} \alpha_{ij}^k s(t - \tau_{ij}^k) + \sum_{\ell=1}^{N_J} \gamma_{i\ell} \sqrt{P_\ell^J} v_{i\ell j}(t) + n_{ij}(t) \quad (1)$$

for $t \in [0, T_{\text{obs}}]$, $i \in \{1, \ldots, N_T\}$ and $j \in \mathcal{A}_i$, where T_{obs} is the observation time, α_{ij}^k and τ_{ij}^k denote, respectively, the

[1] The generalization to the three-dimensional scenario is straightforward, but is not explored in this study.

[2] Although it is common to model the jammer noise as Gaussian [28]–[30], a different problem arises when the jammer nodes transmit signals that are similar to the ranging signals between the target and anchor nodes [31], [32]. However, such a scenario requires information about the ranging signals to be available at the jammer nodes (see Section VI).

amplitude and delay of the kth multipath component between anchor node j and target node i, L_{ij} is the number of paths between target node i and anchor node j, and $\gamma_{i\ell}$ represents the channel coefficient between target node i and the ℓth jammer node, which has a transmit power of P_ℓ^J. The transmit signal $s(t)$ is known, and the measurement noise $n_{ij}(t)$ and the jammer noise $\sqrt{P_\ell^J}v_{i\ell j}(t)$ are assumed to be independent zero-mean white Gaussian random processes, where the spectral density level of $n_{ij}(t)$ is $N_0/2$ and that of $v_{i\ell j}(t)$ is equal to one. Also, for each target node, $n_{ij}(t)$'s are independent for $j \in \mathcal{A}_i$, and $v_{i\ell j}(t)$'s are independent for $\ell \in \{1, \ldots, N_J\}$ and $j \in \mathcal{A}_i$.[3] The delay τ_{ij}^k is given by

$$\tau_{ij}^k \triangleq \frac{\|\boldsymbol{y}_j - \boldsymbol{x}_i\| + b_{ij}^k}{c} \tag{2}$$

with $b_{ij}^k \geq 0$ denoting a range bias and c being the speed of propagation. Set $\mathcal{A}_i$ is partitioned as

$$\mathcal{A}_i \triangleq \mathcal{A}_i^L \cup \mathcal{A}_i^{NL} \tag{3}$$

where $\mathcal{A}_i^L$ and $\mathcal{A}_i^{NL}$ represent the sets of anchors nodes with line-of-sight (LOS) and non-line-of-sight (NLOS) connections to target node i, respectively.

III. Optimal Power Allocation for Jammer Nodes

In this section, the aim is to obtain optimal power allocation strategies for the jammer nodes in order to minimize the localization performance of the system. Two different optimization criteria are considered in terms of the average and the minimum CRLB for the target nodes. To that aim, we first present the CRLB expressions for the target nodes.

A. CRLB for Location Estimation of Target Nodes

To specify the set of unknown parameters related to target node i, the following vector is defined, which consists of the bias terms in the LOS and NLOS cases [33]:

$$\boldsymbol{b}_{ij} = \begin{cases} \left[b_{ij}^2 \ldots b_{ij}^{L_{ij}}\right]^T, & \text{if } j \in \mathcal{A}_i^L \\ \left[b_{ij}^1 \ldots b_{ij}^{L_{ij}}\right]^T, & \text{if } j \in \mathcal{A}_i^{NL} \end{cases} \tag{4}$$

Based on (4), the unknown parameters related to target node i are defined as [6]

$$\boldsymbol{\theta}_i \triangleq \left[\boldsymbol{x}_i^T \ \boldsymbol{b}_{i\mathcal{A}_i(1)}^T \cdots \boldsymbol{b}_{i\mathcal{A}_i(|\mathcal{A}_i|)}^T \ \boldsymbol{\alpha}_{i\mathcal{A}_i(1)}^T \cdots \boldsymbol{\alpha}_{i\mathcal{A}_i(|\mathcal{A}_i|)}^T\right]^T \tag{5}$$

where $\mathcal{A}_i(j)$ denotes the jth element of set $\mathcal{A}_i$, $|\mathcal{A}_i|$ represents the number of elements in $\mathcal{A}_i$, and $\boldsymbol{\alpha}_{ij} = [\alpha_{ij}^1 \cdots \alpha_{ij}^{L_{ij}}]^T$. (It is assumed that each target node knows the total noise level.)

The CRLB, which provides a lower bound on the variance of any unbiased estimator, for location estimation is given by [34]

$$\mathbb{E}\left\{\|\hat{\boldsymbol{x}}_i - \boldsymbol{x}_i\|^2\right\} \geq \text{tr}\left\{\left[\boldsymbol{F}_i^{-1}\right]_{2\times 2}\right\}, \tag{6}$$

where $\hat{\boldsymbol{x}}_i$ denotes an unbiased estimate of the location of target node i, tr represents the trace operator, and $\boldsymbol{F}_i$ is the Fisher information matrix for vector $\boldsymbol{\theta}_i$. Following the steps taken in [6], $\left[\boldsymbol{F}_i^{-1}\right]_{2\times 2}$ can be expressed as

$$\left[\boldsymbol{F}_i^{-1}\right]_{2\times 2} = \boldsymbol{J}_i(\boldsymbol{x}_i, \boldsymbol{p}^J)^{-1} \tag{7}$$

where the equivalent Fisher information matrix $\boldsymbol{J}_i(\boldsymbol{x}_i, \boldsymbol{p}^J)$ in the absence of prior information about the location of the target node is calculated as (see [6, Th. 1] for details)

$$\boldsymbol{J}_i(\boldsymbol{x}_i, \boldsymbol{p}^J) = \sum_{j\in\mathcal{A}_i^L} \frac{\lambda_{ij}}{N_0/2 + \boldsymbol{a}_i^T \boldsymbol{p}^J} \boldsymbol{\phi}_{ij}\boldsymbol{\phi}_{ij}^T \tag{8}$$

with

$$\lambda_{ij} \triangleq \frac{4\pi^2\beta^2|\alpha_{ij}^1|^2 \int_{-\infty}^{\infty}|S(f)|^2 df}{c^2}(1 - \xi_{ij}), \tag{9}$$

$$\boldsymbol{a}_i \triangleq \left[|\gamma_{i1}|^2 \cdots |\gamma_{iN_J}|^2\right]^T, \tag{10}$$

$$\boldsymbol{p}^J \triangleq \left[P_1^J \cdots P_{N_J}^J\right]^T, \tag{11}$$

$$\boldsymbol{\phi}_{ij} \triangleq \left[\cos\varphi_{ij} \ \ \sin\varphi_{ij}\right]^T. \tag{12}$$

In (9), β is the effective bandwidth, which is expressed as

$$\beta = \sqrt{\frac{\int_{-\infty}^{\infty} f^2|S(f)|^2 df}{\int_{-\infty}^{\infty}|S(f)|^2 df}}, \tag{13}$$

with $S(f)$ denoting the Fourier transform of $s(t)$, and the path-overlap coefficient ξ_{ij} is a non-negative number between zero and one, i.e., $0 \leq \xi_{ij} \leq 1$ [14]. Also, in (12), φ_{ij} denotes the angle between target node i and anchor node j. In addition, it is assumed that the elements of $\boldsymbol{a}_i$ are non-zero (i.e., strictly positive) for $i \in \{1, 2, \ldots, N_T\}$. It is noted from (8) that the effects of the jammer nodes appear as the second term in the denominator since the jammer nodes transmit Gaussian noise.

Remark 1: In this section, the jammer nodes are assumed to know the locations of the anchor and target nodes and the channel gains. In practice, this information may not be available to jammer nodes completely. However, this assumption is employed in this section for two purposes: (i) to obtain initial results that can form a basis for further studies on the problem of optimal power allocation of jammer nodes in localization systems, which has not been studied before (see Section IV for extensions in the presence of parameter uncertainty), (ii) to provide theoretical limits on the best achievable performance of jammer nodes; that is, if the jammer nodes are smart and can learn all the environmental parameters, the localization accuracy obtained in this study can be achieved; otherwise, the localization accuracy is bounded by the obtained results.

B. Optimal Power Allocation Strategies

Before the introduction of the proposed optimal power allocation strategies, the dependence of the CRLB for target node i (that is, the trace of $\boldsymbol{J}_i(\boldsymbol{x}_i, \boldsymbol{p}^J)^{-1}$ in (7)) on the power vector of the jammer nodes, $\boldsymbol{p}^J$, is specified.

[3] It is assumed that the anchor nodes transmit at different time intervals to prevent interference at the target nodes [6]. During these time intervals, the channel coefficient between a jammer node and a target node is assumed to be constant.

Lemma 1: Consider the equivalent Fisher information matrix in (8). The trace of the inverse of $\boldsymbol{J}_i(\boldsymbol{x}, \boldsymbol{p}^J)$ is an affine function with respect to $\boldsymbol{p}^J$.

Proof: From the definition of the equivalent Fisher information matrix in (8), it can be shown that

$$\begin{aligned}
&\mathrm{tr}\left\{\boldsymbol{J}_i(\boldsymbol{x}_i, \boldsymbol{p}^J)^{-1}\right\} \\
&\quad = \mathrm{tr}\left\{\left[\sum_{j\in\mathcal{A}_i^L} \frac{\lambda_{ij}}{N_0/2 + \boldsymbol{a}_i^T \boldsymbol{p}^J}\boldsymbol{\phi}_{ij}\boldsymbol{\phi}_{ij}^T\right]^{-1}\right\} \\
&\quad = (N_0/2 + \boldsymbol{a}_i^T \boldsymbol{p}^J)\,\mathrm{tr}\left\{\left[\sum_{j\in\mathcal{A}_i^L} \lambda_{ij}\boldsymbol{\phi}_{ij}\boldsymbol{\phi}_{ij}^T\right]^{-1}\right\} \\
&\quad \triangleq r_i\,\boldsymbol{a}_i^T \boldsymbol{p}^J + r_i N_0/2 \qquad (14)
\end{aligned}$$

where

$$r_i \triangleq \mathrm{tr}\left\{\left[\sum_{j\in\mathcal{A}_i^L} \lambda_{ij}\boldsymbol{\phi}_{ij}\boldsymbol{\phi}_{ij}^T\right]^{-1}\right\}. \qquad (15)$$

Hence, $\mathrm{tr}\left\{\boldsymbol{J}_i(\boldsymbol{x}_i, \boldsymbol{p}^J)^{-1}\right\}$ is an affine function with respect to vector $\boldsymbol{p}^J$. ∎

Lemma 1 states that the CRLB for each target node is an affine function of the power vector of the jammer nodes. Based on this result, two approaches are proposed in the following for optimal power allocation of jammer nodes, and convex (in fact, linear) optimization problems, which can efficiently be solved, are obtained.

Remark 2: The use of the CRLB as a metric for localization performance can be justified as follows. As discussed in [35], for sufficiently large signal-to-noise ratios (SNRs) and/or effective bandwidths, the maximum likelihood (ML) location estimator becomes approximately unbiased and efficient, i.e., it achieves a mean-squared error (MSE) that is close to the CRLB. For other scenarios, the CRLB may not be a very tight bound for MSEs of ML estimators [36], [37]. Therefore, when the power allocation strategy for the jammer nodes is optimized according to a CRLB based objective function, the CRLBs corresponding to the optimized value of the specific objective function can be considered to provide performance bounds for the MSEs of the target nodes. The difference between the exact localization performance of a target node and the CRLB depends on the SNR and effective bandwidth parameters. Another motivation for the use of the CRLB metric is that the CRLB expressions lead to optimization problems that have desirable structures, which lead to closed form expressions or facilitate theoretical analyses.

Remark 3: In addition to the powers of the jammer nodes, the effectiveness of jamming depends also on the network geometry, that is, the locations of the anchor, target, and jammer nodes. This dependence can be observed from the CRLB expression in (14) through the r_i and $\boldsymbol{a}_i$ terms. In particular, r_i in (15) depends on the locations of the anchor and target nodes via the λ_{ij} and $\boldsymbol{\phi}_{ij}$ parameters in (9) and (12), respectively, where the dependence of λ_{ij} on the locations (network geometry) is due to the channel coefficient and the path-overlap coefficient terms. On the other hand, the dependence of the CRLB in (14) on the jammer locations is via the $\boldsymbol{a}_i$ parameter in (10), which consists of the channel power gains between a target node and all the jammer nodes. In this study, the aim is to perform the optimal power allocation for the jammer nodes for a given network geometry (see Section VI for extensions and future work).

1) Optimal Power Allocation Based on Average CRLB: In the first proposed approach, the average CRLB for the target nodes is to be maximized under total and peak power constraints on the jammer nodes, which leads to the following formulation:

$$\begin{aligned}
&\underset{\boldsymbol{p}^J}{\text{maximize}} \ \frac{1}{N_T}\sum_{i=1}^{N_T}\mathrm{tr}\left\{\boldsymbol{J}_i(\boldsymbol{x}_i, \boldsymbol{p}^J)^{-1}\right\} \\
&\text{subject to } \mathbf{1}^T\boldsymbol{p}^J \le P_T \\
&\qquad 0 \le P_\ell^J \le P_\ell^{\text{peak}}, \quad \ell = 1, 2, \ldots, N_J \qquad (16)
\end{aligned}$$

where $P_T < \infty$ is the total available jammer power and P_ℓ^{peak} is the maximum allowed power (peak power) for jammer node ℓ.[4] From (14), the problem in (16) can be expressed as a linear programming (LP) problem as follows [38]:

$$\begin{aligned}
&\underset{\boldsymbol{p}^J}{\text{maximize}} \ \left(\sum_{i=1}^{N_T} r_i\,\boldsymbol{a}_i^T\right)\boldsymbol{p}^J \\
&\text{subject to } \mathbf{1}^T\boldsymbol{p}^J \le P_T \\
&\qquad 0 \le P_\ell^J \le P_\ell^{\text{peak}}, \quad \ell = 1, 2, \ldots, N_J \qquad (17)
\end{aligned}$$

where the scaling term $1/N_T$ and the constant term $(N_0/2)\sum_{i=1}^{N_T} r_i$ are omitted since they have no effects on the optimal value of the power vector of the jammer nodes.

The following proposition presents the solution of (17):

Proposition 2: Define $\boldsymbol{w} \triangleq \sum_{i=1}^{N_T} r_i\,\boldsymbol{a}_i$, and let $h(j)$ denote the index of the jth largest element of vector $\boldsymbol{w}$, where $j = 1, \ldots, N_J$.[5] Then, the elements of the solution $\boldsymbol{p}_{\text{opt}}^J$ of (17) can be expressed as

***Scheme 1*:**

$$\boldsymbol{p}_{\text{opt}}^J(h(j)) = \min\left\{P_T - \sum_{l=1}^{j-1}\boldsymbol{p}_{\text{opt}}^J(h(l)),\, P_{h(j)}^{\text{peak}}\right\} \qquad (18)$$

for $j = 1, \ldots, N_J$, where $\boldsymbol{p}_{\text{opt}}^J(h(j))$ represents the $h(j)$th element of $\boldsymbol{p}_{\text{opt}}^J$, and $\sum_{l=1}^{0}(\cdot)$ is defined as zero.

Proof: Optimization problems in the form of (17) have been studied in the OFDM and MIMO literature; e.g., [39] and [40]. The expression in (18) can be derived in a similar fashion to the derivation in [39]. First, it is observed that the elements of $\boldsymbol{w}$ defined in the proposition are all positive, which is based on the definitions of $\boldsymbol{a}_i$ and r_i in (10) and (15), respectively.[6] In addition, from the

[4] It is assumed that the jammer nodes are controlled by a central unit, which performs optimal power allocation under total and peak power constraints.

[5] For example, if $\boldsymbol{w} = [2\ 5\ 1\ 3\ 2]^T$, then $h(1) = 2$, $h(2) = 4$, $h(3) = 1$, $h(4) = 5$, and $h(5) = 3$.

[6] Note from (14) and (15) that the CRLB in the absence of jammer nodes (that is, for $\boldsymbol{p}^J = \mathbf{0}$ in (14)) is given by $r_i N_0/2$, which is a positive quantity.

definition of $\boldsymbol{w}$, the objective function in (17) can be expressed as $\boldsymbol{w}^T \boldsymbol{p}^J$. Then, under the constraints in (17), $\boldsymbol{w}^T \boldsymbol{p}^J$ can be maximized by assigning the maximum allowed power (i.e., $\min\{P_T, P_{h(1)}^{\text{peak}}\}$) to the jammer node corresponding to the largest element of $\boldsymbol{w}$ (that is, the $h(1)$th element), the remaining power (subject to the peak power constraint) to the jammer node corresponding to the second largest element of $\boldsymbol{w}$ (that is, the $h(2)$th element), and so on. Hence, the solution in (18) can be obtained. ∎

Proposition 2 implies that Scheme 1, which aims to maximize the average CRLB of the target nodes, tends to assign all the power to a single jammer node that can cause the largest increase in the average CRLB. If the peak power limit is sufficiently high, then the total power P_T is assigned to that jammer node (hence, no power is allocated to the other jammer nodes). Otherwise, that jammer node operates at its peak power limit, and the remaining power is assigned to the other jammer node(s) based on the same logic, as formulated in (18).

It is noted that Scheme 1 can be regarded to provide a counterpart of the waterfilling algorithm for capacity maximization over fading channels [40]. In the waterfilling algorithm, a power level of $1/\vartheta_0 - 1/\vartheta$ is assigned for an SNR of ϑ, where $\vartheta \geq \vartheta_0$ with ϑ_0 denoting a threshold obtained from the average power constraint [40]; hence, the assigned power level increases with the SNR. On the other hand, Scheme 1 tends to allocate the whole power to a jammer node that can cause the largest increase in the total CRLB, as stated in (18). If the peak power limit of that jammer node is lower than the total power limit, then the jammer node(s) that can cause the second (third,...) largest increase in the total CRLB are employed.

2) Optimal Power Allocation Based on Minimum CRLB: The second proposed approach is to design the power allocation strategy of the jammer nodes in order to maximize the best accuracy (i.e., the minimum CRLB) of the target nodes, which leads to the following formulation:

$$\begin{aligned} \underset{\boldsymbol{p}^J}{\text{maximize}} \quad & \min_{i\in\{1,2,\ldots,N_T\}} \text{tr}\left\{\boldsymbol{J}_i(\boldsymbol{x}_i, \boldsymbol{p}^J)^{-1}\right\} \\ \text{subject to} \quad & \mathbf{1}^T \boldsymbol{p}^J \leq P_T \\ & 0 \leq P_\ell^J \leq P_\ell^{\text{peak}}, \quad \ell = 1, 2, \ldots, N_J \end{aligned} \tag{19}$$

Based on (14), the problem in (19) in the epigraph form can be expressed as the following LP problem after some manipulation [38]:

***Scheme 2*:**

$$\begin{aligned} \underset{\boldsymbol{p}^J, s}{\text{maximize}} \quad & s \\ \text{subject to} \quad & s - r_i \boldsymbol{a}_i^T \boldsymbol{p}^J - r_i \frac{N_0}{2} \leq 0, \quad i = 1, 2, \ldots, N_T \\ & \mathbf{1}^T \boldsymbol{p}^J \leq P_T \\ & 0 \leq P_\ell^J \leq P_\ell^{\text{peak}}, \quad \ell = 1, 2, \ldots, N_J \end{aligned} \tag{20}$$

where an auxiliary variable s and a new set of constraints are introduced in order to obtain an equivalent problem to (19) in terms of the optimal value of $\boldsymbol{p}^J$.

It is noted from (20) that the computational complexity of the optimal power allocation strategy according to Scheme 2 is quite low in general. In addition, further computational complexity reduction can be achieved via the theoretical results in the remainder of this section.

The following result presents a feature of the optimal solution for Scheme 2, which can be proved based on (14), (19), and the fact that $\boldsymbol{a}_i \succ \mathbf{0}$ (i.e., each element of $\boldsymbol{a}_i$ is positive) for $i \in \{1, 2, \ldots, N_T\}$.

Lemma 3: Assume that $P_T < \sum_{\ell=1}^{N_J} P_\ell^{\text{peak}}$. Then, the solution of (19) (equivalently, (20)) always operates at the total power limit; that is, $\mathbf{1}^T \boldsymbol{p}_{\text{opt}}^J = P_T$.

In practice, the total power limit is related to the power/energy consumption of the system, which is set according to certain cost considerations. On the other hand, the peak power limit is commonly a hardware constraint, which specifies the maximum power/amplitude level that can be generated by a transmitter circuitry [41]. The assumption in Lemma 3 can be regarded as a common scenario for practical systems. Hence, the optimal power allocation strategy according to Scheme 2 operates at the total power limit in realistic scenarios as can be expected.

In the following proposition, the solution for Scheme 2 is characterized under certain conditions.

Proposition 4: Suppose that target node k uniquely has the minimum CRLB among all the target nodes in the absence of jammer nodes. Then, the optimal power allocation strategy for Scheme 2 is to allocate all the power to jammer node b_k (assuming that $P_{b_k}^{\text{peak}} \geq P_T$), where

$$b_k = \underset{\ell\in\{1,\ldots,N_J\}}{\arg\max} \; |\gamma_{k\ell}|^2, \tag{21}$$

if the total power limit satisfies $P_T \leq P_T^{(k)}$, where

$$P_T^{(k)} = \min_{i\in\{1,\ldots,N_T\}\setminus\{k\}} P_T^{(i,k)} \tag{22}$$

with

$$P_T^{(i,k)} = \begin{cases} \dfrac{(r_i - r_k)N_0/2}{r_k|\gamma_{kb_k}|^2 - r_i|\gamma_{ib_k}|^2}, & \text{if } r_i|\gamma_{ib_k}|^2 < r_k|\gamma_{kb_k}|^2 \\ \infty, & \text{otherwise.} \end{cases} \tag{23}$$

Proof: From (14), the CRLB for target node i in the absence of jammer nodes is given by $r_i N_0/2$ for $i \in \{1, \ldots, N_T\}$. Therefore, under the assumption in the proposition, r_k is the unique minimum of set $\{r_1, \ldots, r_{N_T}\}$. Hence, there exists $\Delta > 0$ such that the minimum of $\text{CRLB}_1, \ldots, \text{CRLB}_{N_T}$ for $P_T \in [0, \Delta]$ is equal to CRLB_k for all possible $\boldsymbol{p}^J$, where $\text{CRLB}_i = r_i \boldsymbol{a}_i^T \boldsymbol{p}^J + r_i N_0/2$ as defined in (14). Since Scheme 2 aims to maximize the minimum CRLB, it should maximize the CRLB of target node k, i.e., CRLB_k, for $P_T \in [0, \Delta]$, which can be expressed, based on (10), (11), and (14), as

$$r_k\left(|\gamma_{k1}|^2 P_1^J + \cdots + |\gamma_{kN_J}|^2 P_{N_J}^J\right) + r_k N_0/2. \tag{24}$$

The maximization of CRLB_k in (24) is achieved by assigning all the power to the jammer node that has the best channel gain; that is, the maximum of $|\gamma_{kj}|^2$ for $j \in \{1, \ldots, N_J\}$. In other words, all the power, P_T, is allocated to jammer

node b_k as specified in (21). For this power allocation strategy, the CRLB expressions become

$$\text{CRLB}_i = r_i |\gamma_{ib_k}|^2 P_T + r_i N_0/2 \tag{25}$$

for $i = 1, \ldots, N_T$. As long as CRLB_k is the minimum CRLB, the strategy that assigns all the power to jammer node b_k is optimal according to Scheme 2. In order to specify the range of P_T values for which target node k has the minimum CRLB, the first intersection point of CRLB_k with other CRLB curves can be calculated. It is noted from (25) that the CRLB expressions correspond to straight lines with respect to P_T, and CRLB_k intersects with CRLB_i at total power level

$$\frac{(r_i - r_k)N_0/2}{r_k|\gamma_{kb_k}|^2 - r_i|\gamma_{ib_k}|^2} \tag{26}$$

if $r_i|\gamma_{ib_k}|^2 < r_k|\gamma_{kb_k}|^2$ and does not intersect otherwise. Therefore, the minimum of the intersection points in (26) for all $i \in \{i \in \{1, \ldots, N_T\} \,|\, i \neq k \text{ and } r_i|\gamma_{ib_k}|^2 < r_k|\gamma_{kb_k}|^2\}$ specifies the value of P_T before which the optimal strategy for Scheme 2 is to assign all the power to the b_kth jammer node. Hence, the expressions in (22) and (23) are obtained by also defining the intersection point to be infinity when two curves do not intersect.[7] ■

Proposition 4 describes a closed-form solution of the optimal power allocation strategy for Scheme 2 when the total power limit in (19) (equivalently, in (20)) is lower than or equal to a certain value specified by (22) and (23). Based on the statements in the proposition, the optimal power allocation strategy for Scheme 2 can be specified as follows: First, the r_i terms in (15) are calculated for all the target nodes, and the target node with the minimum r_i, say the kth one, is determined. (It is assumed that only one target node achieves the minimum value.) Then, the channel gains between the kth target node and the jammer nodes are compared, and the jammer node that has the largest channel gain (that is, the best channel condition) with the kth target node is found as in (21).[8] Finally, the optimal power allocation strategy according to Scheme 2 is specified by sending the whole power, P_T, from the jammer node that has the best channel condition with the k target node if $P_T \leq P_T^{(k)}$ as specified in (22) and (23). For $P_T > P_T^{(k)}$, the problem in (20) needs to be solved.

If there exist multiple target nodes that have the minimum CRLB in the absence of jammer nodes, Proposition 4 can be extended under certain conditions as follows: Let target nodes $k_1, \ldots, k_{N_M}$ achieve the minimum CRLB in the absence of jamming and let b_k in (21) denote the jammer node that has the best channel condition with target node k, where $k \in \{k_1, \ldots, k_{N_M}\}$. Assume that there exists $k^* \in \{k_1, \ldots, k_{N_M}\}$ such that $|\gamma_{k^* b_{k^*}}| \leq |\gamma_{m b_{k^*}}|$, $\forall m \in \{k_1, \ldots, k_{N_M}\} \setminus \{k^*\}$. Then, assigning all the power to jammer node b_{k^*} is optimal for $P_T \leq P_T^{(k^*)}$ (assuming that $P_{b_{k^*}}^{\text{peak}} \geq P_T$), where $P_T^{(k^*)}$ is given by

$$P_T^{(k^*)} = \min_{i \in \{1,\ldots,N_T\} \setminus \{k_1,\ldots,k_{N_M}\}} P_T^{(i,k^*)}$$

with $P_T^{(i,k^*)}$ being as in (23). (This claim can be proved very similarly to Proposition 4.)

In the absence of peak power limits on the jammer nodes (i.e., when the peak power limits in (19) are ineffective), the following result states an upper limit on the number of jammer nodes that should be employed for Scheme 2.

Proposition 5: Assume that r_i in (15) is finite for $i \in \{1, \ldots, N_T\}$. In the absence of peak power constraints, the solution of (19), denoted by $\boldsymbol{p}_{\text{opt}}^J$, can be expressed to have at most N_T non-zero elements (that is, non-zero power is allocated to at most N_T jammer nodes), where N_T is the number of target nodes.

Proof: In the absence of peak power constraints, the problem in (19) can be expressed, based on (14) and Lemma 3, as

$$\begin{aligned} &\underset{\boldsymbol{p}^J}{\text{maximize}} \quad \min_{i \in \{1,2,\ldots,N_T\}} r_i \, \boldsymbol{a}_i^T \boldsymbol{p}^J + r_i N_0/2 \\ &\text{subject to } \mathbf{1}^T \boldsymbol{p}^J = P_T \end{aligned} \tag{27}$$

By introducing the scaled version of the power levels of the jammer nodes as $\tilde{\boldsymbol{p}}^J \triangleq \boldsymbol{p}^J / P_T$, the objective function in (27) can be stated as

$$\left(P_T \, r_i \, \boldsymbol{a}_i + r_i \, \frac{N_0}{2} \mathbf{1} \right)^T \tilde{\boldsymbol{p}}^J \triangleq \boldsymbol{d}_i^T \tilde{\boldsymbol{p}}^J \tag{28}$$

for $i \in \{1, \ldots, N_T\}$, where $\mathbf{1}^T \tilde{\boldsymbol{p}}^J = 1$ and $\tilde{\boldsymbol{p}}^J \succeq \mathbf{0}$. In other words, for a given power allocation vector for the jammer nodes, the objective function for target node i is equal to the *convex combination* of the elements of $\boldsymbol{d}_i$. Next, vector $\tilde{\boldsymbol{d}}_\ell$ is defined as $\tilde{\boldsymbol{d}}_\ell \triangleq [d_{1,\ell} \; d_{2,\ell} \cdots d_{N_T,\ell}]^T$ for $\ell \in \{1, \ldots, N_J\}$, where $d_{i,\ell}$ denotes the ℓth element of $\boldsymbol{d}_i$ specified in (28). The set consisting of $\tilde{\boldsymbol{d}}_\ell$'s is represented by $\mathcal{U}$; that is, $\mathcal{U} = \{\tilde{\boldsymbol{d}}_1, \tilde{\boldsymbol{d}}_2, \ldots, \tilde{\boldsymbol{d}}_{N_J}\}$. It is noted that the values of the objective function in (28) for any given jammer power vector, i.e., $\boldsymbol{d}_1^T \tilde{\boldsymbol{p}}^J, \ldots, \boldsymbol{d}_{N_T}^T \tilde{\boldsymbol{p}}^J$, correspond to a certain convex combination of the elements of $\mathcal{U}$. In other words, the convex hull of set $\mathcal{U}$ contains the values of the objective functions for all possible power allocation strategies. Therefore, the *optimal* power allocation strategy obtained as the solution of (27) should correspond to a point in the convex hull of $\mathcal{U}$, as well. In addition, since a maximization problem is considered in (27), the optimal power allocation strategy should correspond to a point on the *boundary* of the convex hull. (For any point in the *interior* of the convex hull, there exists an open ball centered at that point that is completely contained in the convex hull, which implies that the objective functions in (28) (equivalently, (27)) can simultaneously be increased to achieve a larger minimum value; hence, the optimal solution cannot correspond to an interior point.) Then, Carathéodory's theorem [42] is invoked, which states that any point on the boundary of the convex hull of $\mathcal{U}$ can be represented by the convex combination of at most $\dim(\mathcal{U})$ elements in $\mathcal{U}$. By noting that $\mathcal{U} \subset \mathbb{R}^{N_T}$, it is then concluded that an optimal power allocation strategy for the jammer nodes

[7] If all the $P_T^{(i,k)}$ terms are infinity in (23), then the strategy specified in Proposition 4 becomes the optimal approach for Scheme 2 for all values of P_T.

[8] If there are multiple jammer nodes with the largest channel gain with respect to the kth target node, then one of them can simply be chosen.

can be represented by the convex combination of at most N_T elements in set $\mathcal{U}$, corresponding to at most N_T non-zero elements in $\tilde{\boldsymbol{p}}^J$ (equivalently, $\boldsymbol{p}^J$). ■

Proposition 5 states that when the peak power constraints are not effective, it is not necessary for Scheme 2 to employ more jammer nodes than the number of target nodes. For example, in the presence of two target nodes and three jammer nodes, an optimal power allocation strategy according to Scheme 2 can always be obtained by assigning non-zero power to at most two jammer nodes in the absence of peak power constraints. Based on Propositions 4 and 5, it can also be shown that, in the absence of peak power constraints, the optimal power allocation strategy according to Scheme 2 allocates non-zero power to at most N_M jammer nodes for low values of P_T, where N_M is the number of target nodes that have the minimum CRLB in the absence of jammer nodes.

A related result to Proposition 5 is presented in [43, Th. 1] for the optimal power allocation of anchor nodes for the aim of minimizing the CRLB (in the absence of jammer nodes), and it is shown that the optimal solution can be implemented by transmitting power from at most $\binom{D+1}{2}$ anchor nodes, where D is the dimension of the environment with $D \in \{2, 3\}$. In addition to the difference between the results, both the employed proof techniques and the considered objective functions are different in [43, Th. 1] and in Proposition 5.

Remark 4: Although the LP problems in (17) and (20) can directly be solved with the standard solvers for LP problems [38], the results in Propositions 3.2, 3.4, and 3.5 both facilitate low-complexity implementations and provide important insights about the optimal power allocation strategies.

IV. Robust Power Allocation for Jammer Nodes

In the previous section, the optimal power allocation strategies are developed in the presence of perfect information at the jammer nodes. In practice, jammer nodes can gather information about the localization parameters by various means such as using cameras to learn the locations of the target and anchor nodes, performing measurements from the environment beforehand to form a database for the channel parameters (fingerprinting), and listening to signals between the anchor and target nodes. However, in most cases, the information at the jammer nodes about the localization related parameters cannot be perfect. Therefore, it is important to design power allocation strategies for jammer nodes that are robust against uncertainties in localization related parameters.

From the perspective of the jammer nodes, uncertainties can exist in the positions of the target and anchor nodes, the channel gains between the target and anchor nodes, and the channel gains between the jammer and target nodes. For CRLB based optimization approaches, all these uncertainties can be modeled as uncertainties in r_i and $\boldsymbol{a}_i$ for target node i since the CRLB is given by $r_i\, \boldsymbol{a}_i^T\, \boldsymbol{p}^J + r_i N_0/2$ for $i \in \{1, \ldots, N_T\}$ as stated in (14), where $\boldsymbol{a}_i$ is specified by (10) and r_i is defined in (15), which depends on λ_{ij} in (9) and $\boldsymbol{\phi}_{ij}$ in (12). Let $\mathcal{R}_i$ and $\mathcal{C}_i$ denote the uncertainty sets for r_i and $\boldsymbol{a}_i$, respectively. Then, the following robust optimization problems are proposed:

Scheme 1-R:

$$\begin{aligned} \underset{\boldsymbol{p}^J}{\text{maximize}} \;& \frac{1}{N_T} \sum_{i=1}^{N_T} \min_{\substack{r_i \in \mathcal{R}_i \\ \boldsymbol{a}_i \in \mathcal{C}_i}} r_i \left(\boldsymbol{a}_i^T \boldsymbol{p}^J + N_0/2 \right) \\ \text{subject to } & \mathbf{1}^T \boldsymbol{p}^J \le P_T \\ & 0 \le P_\ell^J \le P_\ell^{\text{peak}}, \quad \ell = 1, 2, \ldots, N_J \end{aligned} \tag{29}$$

Scheme 2-R:

$$\begin{aligned} \underset{\boldsymbol{p}^J}{\text{maximize}} \;& \min_{i \in \{1,\ldots,N_T\}} \min_{\substack{r_i \in \mathcal{R}_i \\ \boldsymbol{a}_i \in \mathcal{C}_i}} r_i \left(\boldsymbol{a}_i^T \boldsymbol{p}^J + N_0/2 \right) \\ \text{subject to } & \mathbf{1}^T \boldsymbol{p}^J \le P_T \\ & 0 \le P_\ell^J \le P_\ell^{\text{peak}}, \quad \ell = 1, 2, \ldots, N_J \end{aligned} \tag{30}$$

It is noted that the problems in (29) and (30), which consider the minimum (worst-case from a jamming perspective) CRLBs over the uncertainty sets, can be regarded as the robust versions of Scheme 1 and Scheme 2 in Section III.

In order to simplify the problems in (29) and (30), the following equation is stated first:

$$\min_{\substack{r_i \in \mathcal{R}_i \\ \boldsymbol{a}_i \in \mathcal{C}_i}} r_i \left(\boldsymbol{a}_i^T \boldsymbol{p}^J + N_0/2 \right) = \min_{\boldsymbol{a}_i \in \mathcal{C}_i} r_i^{\min} \left(\boldsymbol{a}_i^T \boldsymbol{p}^J + N_0/2 \right) \tag{31}$$

where $r_i^{\min} \triangleq \min_{r_i \in \mathcal{R}_i} r_i$, which follows from the fact that both r_i and $(\boldsymbol{a}_i^T \boldsymbol{p}^J + N_0/2)$ are always non-negative. Next, the uncertainty set $\mathcal{C}_i$ is specified as a linear uncertainty as follows:

$$\mathcal{C}_i = \left[|\gamma_{i1}|^2_{\min}, |\gamma_{i1}|^2_{\max} \right] \times \cdots \times \left[|\gamma_{iN_J}|^2_{\min}, |\gamma_{iN_J}|^2_{\max} \right] \tag{32}$$

where $\times$ denotes the Cartesian product, and $|\gamma_{i\ell}|^2_{\min}$ and $|\gamma_{i\ell}|^2_{\max}$ represent the minimum and maximum values of $|\gamma_{i\ell}|^2$, respectively (cf. (10)). It should be emphasized that the use of linear uncertainty sets as in (32) is a common approach for developing robust algorithms; e.g., see [14]. From (32), the expression in (31) is simplified as

$$\min_{\boldsymbol{a}_i \in \mathcal{C}_i} r_i^{\min} \left(\boldsymbol{a}_i^T \boldsymbol{p}^J + N_0/2 \right) = r_i^{\min} \left(\tilde{\boldsymbol{a}}_i^T \boldsymbol{p}^J + N_0/2 \right) \tag{33}$$

where $\tilde{\boldsymbol{a}}_i^T \triangleq [|\gamma_{i1}|^2_{\min} \cdots |\gamma_{iN_J}|^2_{\min}]$.

Based on (31) and (33), the optimization problems in (29) and (30) can be expressed, respectively, as

$$\begin{aligned} \underset{\boldsymbol{p}^J}{\text{maximize}} \;& \frac{1}{N_T} \sum_{i=1}^{N_T} r_i^{\min} \left(\tilde{\boldsymbol{a}}_i^T \boldsymbol{p}^J + N_0/2 \right) \\ \text{subject to } & \mathbf{1}^T \boldsymbol{p}^J \le P_T \\ & 0 \le P_\ell^J \le P_\ell^{\text{peak}}, \quad \ell = 1, 2, \ldots, N_J \end{aligned} \tag{34}$$

and

$$\begin{aligned} \underset{\boldsymbol{p}^J}{\text{maximize}} \;& \min_{i \in \{1,\ldots,N_T\}} r_i^{\min} \left(\tilde{\boldsymbol{a}}_i^T \boldsymbol{p}^J + N_0/2 \right) \\ \text{subject to } & \mathbf{1}^T \boldsymbol{p}^J \le P_T \\ & 0 \le P_\ell^J \le P_\ell^{\text{peak}}, \quad \ell = 1, 2, \ldots, N_J \end{aligned} \tag{35}$$

Since (34) and (35) are in the same form as the optimization problems for Scheme 1 in (16) and Scheme 2 in (19), respectively, the results in Section III are valid for Scheme 1-R and Scheme 2-R, as well.

Remark 5: Consider scenarios with $P_\ell^{\text{peak}} \geq P_T$ for $\ell = 1, 2, \ldots, N_J$. It is noted from Proposition 2 and the formulation in (34) that Scheme 1 and Scheme 1R result in the same solution when the largest elements of vectors $\sum_{i=1}^{N_T} r_i^{\min} \tilde{\boldsymbol{a}}_i$ and $\sum_{i=1}^{N_T} r_i \boldsymbol{a}_i$ are at the same positions (i.e., have the same indices). Similarly, based on Proposition 4 and the problem in (35), it can be deduced that Scheme 2 and Scheme 2R lead to the same jamming strategy for *small values of* P_T when $\arg\min_{i\in\{1,\ldots,N_T\}} r_i$ is equal to $\arg\min_{i\in\{1,\ldots,N_T\}} r_i^{\min}$ and $\arg\max_{\ell\in\{1,\ldots,N_J\}} |\gamma_{k\ell}|^2 = \arg\max_{\ell\in\{1,\ldots,N_J\}} |\gamma_{k\ell}|^2_{\min}$, where $k = \arg\min_{i\in\{1,\ldots,N_T\}} r_i$.

V. Simulation Results

In this section, performance of the proposed schemes is evaluated through computer simulations. Since there exists no previous work on optimal power allocation for jamming of wireless localization systems, the proposed schemes are compared with uniform power allocation in order to provide intuitive explanations. The uniform power allocation scheme (named Uni-Scheme in the following) assigns equal power levels to all the jammer nodes; that is, $P_\ell^J = P_T/N_J$ for $\ell = 1, \ldots, N_J$, under the assumption that $P_\ell^{\text{peak}} \geq P_T/N_J$, $\forall\, \ell \in \{1, \ldots, N_J\}$.

For the first simulations, a network consisting of four anchor nodes, three target nodes, and three jammer nodes is considered, where the node locations are as illustrated in Fig. 1. It is assumed that each target node has LOS connections to all the anchor nodes. In order to provide a simple and clear comparison of the different power allocation schemes, the total power P_T is normalized as $\bar{P}_T = 2P_T/N_0$ and it is assumed that λ_{ij} in (9) is given by $\lambda_{ij} = 100N_0\|\boldsymbol{x}_i - \boldsymbol{y}_j\|^{-2}/2$; that is, the free space propagation model is considered as in [14]. It is also assumed that $|\gamma_{ij}|^2$ in (10) is expressed as $|\gamma_{ij}|^2 = \|\boldsymbol{x}_i - \boldsymbol{z}_j\|^{-2}$. In addition, N_0 is set to 2, and the peak power limits are taken as $P_\ell^{\text{peak}} = 20$, $\forall\, \ell$.[9] Based on these settings, different schemes are compared in terms of the average, minimum, and individual CRLBs in the following.

The CRLBs of Scheme 1 in (18), Scheme 2 in (20) and Uni-Scheme are plotted in Fig. 2 and Fig. 3. In Fig. 2, the average and the minimum CRLBs are illustrated versus the normalized total power $\bar{P}_T$. It is observed that Scheme 1 and Scheme 2 achieve the best jamming performance in terms of the average CRLB (Fig. 2(a)) and the minimum CRLB (Fig. 2(b)), respectively, which is in accordance with the problem formulations in (16) and (19). Also, Uni-Scheme is not optimal according to either criterion in this example, and significant differences from the optimal performance are observed for large normalized total powers. In other words, the proposed schemes are effective for large total jammer powers

[9] A normalized value for N_0 is used for convenience so that $\bar{P}_T = 2P_T/N_0$ is given by $\bar{P}_T = P_T$. This does not reduce the generality of the results since various values of $\bar{P}_T$ (ranging from zero to sufficiently high values) are considered in the simulations [44].

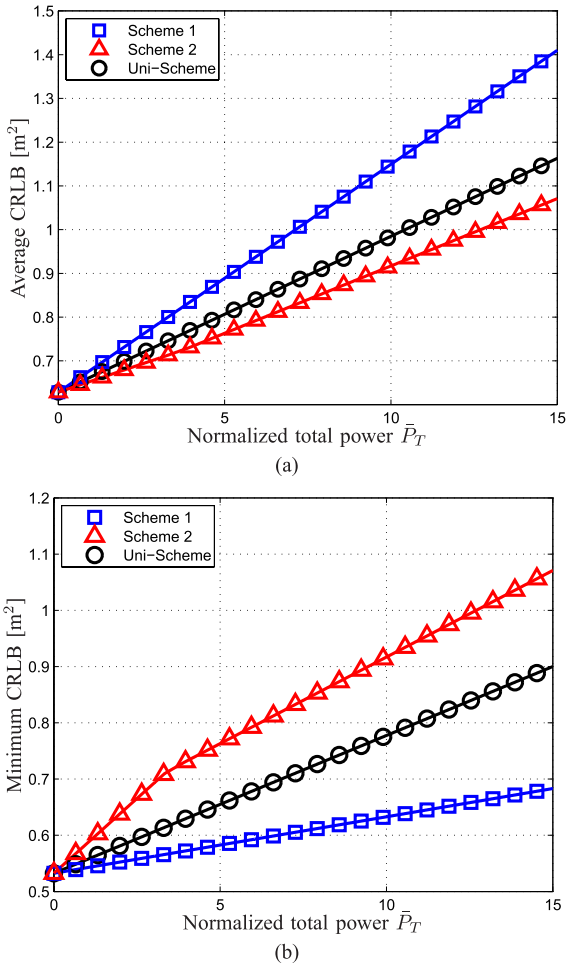

Fig. 2. Comparison of different schemes for power allocation in terms of (a) average CRLB, (b) minimum CRLB for the scenario in Fig. 1.

in this scenario. In Fig. 3, the CRLBs of the three target nodes are plotted versus the normalized total power for different schemes. From the CRLB curves, different behaviors are observed for different target nodes. It is noted that Scheme 1 and Scheme 2 aim to degrade the average (equivalently, total) and the minimum CRLB, respectively, meaning that the individual CRLBs may not always be larger than those for Uni-Scheme.

In Table I, the optimal power allocation strategies are specified for various values of $\bar{P}_T$ according to Scheme 1 and Scheme 2 for the scenario in Fig. 1. It is observed that Scheme 1 always allocates the whole power to jammer node 3 (which is in accordance with (18) in Proposition 2), while Scheme 2 allocates all the power (cf. Lemma 3) either to jammer node 1 or to all the three jammer nodes. From Table I, the claim in Proposition 4 can also be verified. For the considered scenario, the value of $P_T^{(k)}$ in (22) of Proposition 4 can be calculated as 3.3314 with $k = 1$ and $b_k = 1$ in (21). (It is noted from Fig. 3 that target node 1 has the minimum CRLB in the absence of jammer nodes; hence, $k = 1$ in this scenario. Also, since jammer node 1 is the closest jammer node to target node 1, b_k in (21) is equal to 1 due to the distance based channel gain model.) Therefore, for $P_T \leq 3.3314$, the optimal strategy for Scheme 2 is to allocate the whole power

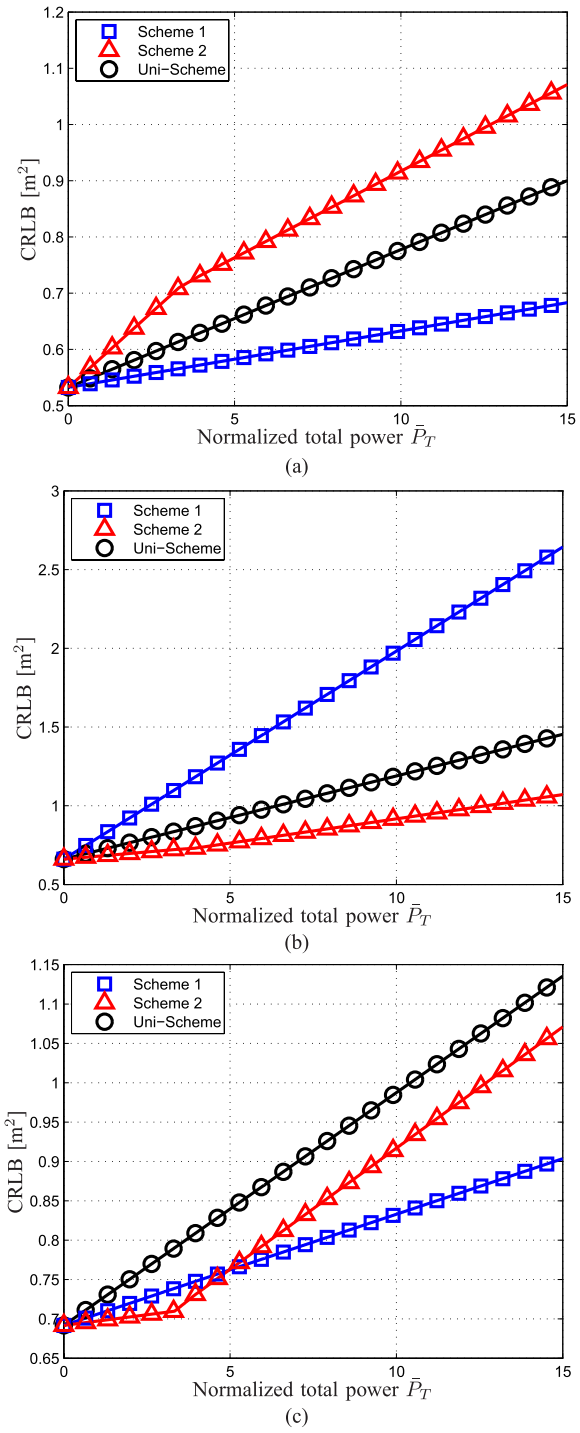

Fig. 3. CRLBs for different schemes of power allocation for (a) Target 1, (b) Target 2, and (c) Target 3 (for the scenario in Fig. 1).

to jammer node 1 in accordance with Proposition 4, which is verified by the results in Table I.

Next, another network with four anchor nodes, two target nodes, and three jammer nodes is considered, as illustrated in Fig. 4. For this network, the average and the minimum CRLBs corresponding to Scheme 1, Scheme 2, and Uni-Scheme are shown in Fig. 5, and the individual CRLBs are presented in Fig. 6. Also, Table II shows the optimal power allocation solutions for Scheme 1 and Scheme 2. Similar observations to those for the network in Fig. 1 are made.

TABLE I

ALLOCATED POWERS TO JAMMER NODES ACCORDING TO SCHEMES 1 AND 2 FOR THE SCENARIO IN FIG. 1

$\bar{P}_T$	Scheme 1			Scheme 2		
	P_1^J	P_2^J	P_3^J	P_1^J	P_2^J	P_3^J
1	0	0	1	1	0	0
2	0	0	2	2	0	0
3	0	0	3	3	0	0
3.3314	0	0	3.3314	3.3314	0	0
4	0	0	4	3.6952	0.2946	0.0102
5	0	0	5	4.1735	0.6729	0.1536
6	0	0	6	4.6518	1.0511	0.2970
7	0	0	7	5.1301	1.4294	0.4405
8	0	0	8	5.6084	1.8077	0.5839
9	0	0	9	6.0867	2.1860	0.7273
10	0	0	10	6.5650	2.5643	0.8707
11	0	0	11	7.0433	2.9426	1.0141
12	0	0	12	7.5216	3.3209	1.1576
13	0	0	13	7.9999	3.6992	1.3010
14	0	0	14	8.4782	4.0774	1.4444
15	0	0	15	8.9565	4.4557	1.5878

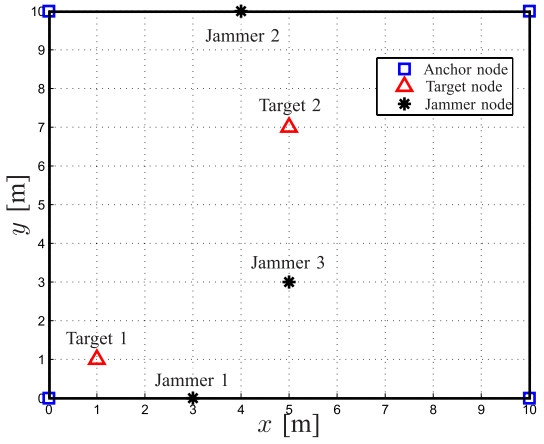

Fig. 4. The network considered in the simulations, where the anchor node positions are [0 0], [10 0], [0 10], and [10 10] m., the target node positions are [1 1] and [5 7] m., and the jammer node positions are [3 0], [4 10], and [5 3] m.

In addition, $P_T^{(k)}$ in Proposition 4 is computed as 4.8952 with $k = 2$ and $b_k = 2$ in (21) for the scenario in Fig. 4, which means that the whole power is allocated to jammer node 2 under Scheme 2 for $P_T \leq 4.8952$ according to Proposition 4. This is verified by the results in Table II, which also shows that the optimal power allocation strategy according to Scheme 2 assigns non-zero power to at most $N_T = 2$ jammer nodes in accordance with Proposition 5.

To provide an example with a high number of nodes, a network with six anchor nodes, five target nodes, and three jammer nodes is considered as illustrated in Fig. 7. Unlike the previous scenarios, the peak power limits are set as $P_\ell^{\text{peak}} = 10$, $\forall\, \ell$, and the jammer nodes are located outside the convex hull of the anchor nodes. In Fig. 8, the average and the minimum CRLBs for each scheme are plotted versus the normalized total power $\bar{P}_T$. In compliance with the previous scenarios, Scheme 1 and Scheme 2 result in the best jamming performance in terms of the average CRLB and the minimum CRLB, respectively, as imposed by the proposed problem formulations. In Table III, the optimal power allocation solutions for Scheme 1 and Scheme 2 are provided. For this scenario, $P_T^{(k)}$ in Proposition 4 is computed as 2.8222 with $k = 1$

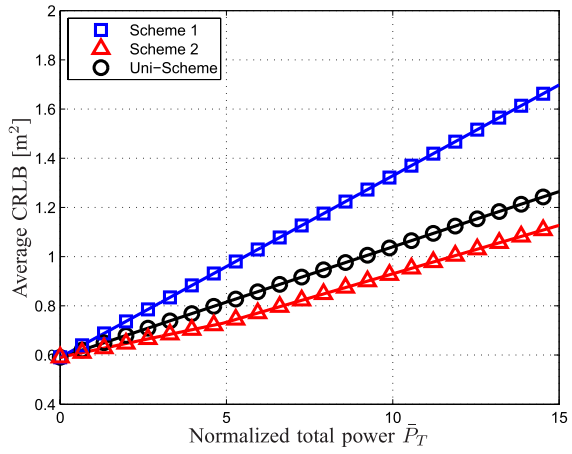

(a)

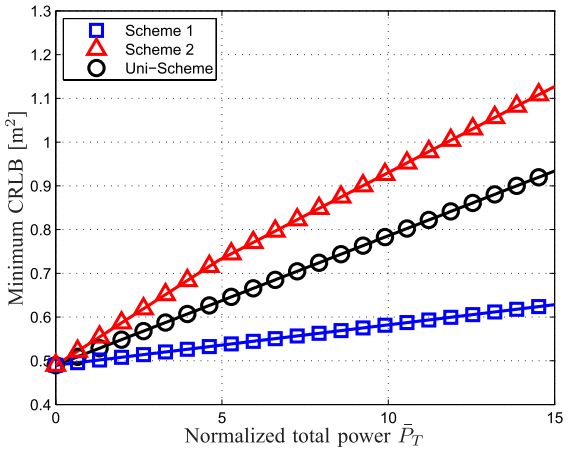

(b)

Fig. 5. Comparison of different schemes for power allocation in terms of (a) average CRLB, (b) minimum CRLB for the scenario in Fig. 4.

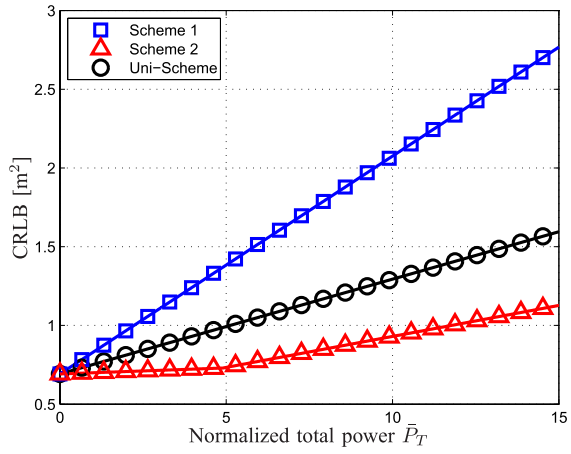

(a)

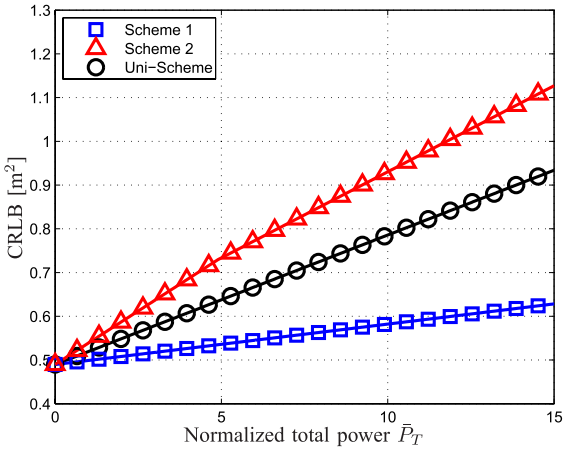

(b)

Fig. 6. CRLBs for different schemes of power allocation for (a) Target 1 and (b) Target 2 (for the scenario in Fig. 4).

TABLE II

ALLOCATED POWERS TO JAMMER NODES ACCORDING TO SCHEMES 1 AND 2 FOR THE SCENARIO IN FIG. 4

$\bar{P}_T$	Scheme 1			Scheme 2		
	P_1^J	P_2^J	P_3^J	P_1^J	P_2^J	P_3^J
1	1	0	0	0	1	0
2	2	0	0	0	2	0
3	3	0	0	0	3	0
4	4	0	0	0	4	0
4.8952	4.8952	0	0	0	4.8952	0
5	5	0	0	0.0254	4.9746	0
6	6	0	0	0.2677	5.7323	0
7	7	0	0	0.5099	6.4901	0
8	8	0	0	0.7522	7.2478	0
9	9	0	0	0.9945	8.0055	0
10	10	0	0	1.2367	8.7633	0
11	11	0	0	1.4790	9.5210	0
12	12	0	0	1.7213	10.2787	0
13	13	0	0	1.9636	11.0364	0
14	14	0	0	2.2058	11.7942	0
15	15	0	0	2.4481	12.5519	0

and $b_k = 1$ in (21), which means that the whole power is allocated to jammer node 1 under Scheme 2 for $P_T \leq 2.8222$ according to Proposition 4, which is as observed in Table III. Unlike the previous scenarios, the power of the jammer node 2 in this scenario reaches out to its peak value $P_2^{\text{peak}} = 10$ for Scheme 1 when $\bar{P}_T \geq 10$, and the power of the jammer node 1 reaches out to its peak value $P_1^{\text{peak}} = 10$ for Scheme 2 when $\bar{P}_T \geq 12.18$.

TABLE III

ALLOCATED POWERS TO JAMMER NODES ACCORDING TO SCHEMES 1 AND 2 FOR THE SCENARIO IN FIG. 7

$\bar{P}_T$	Scheme 1			Scheme 2		
	P_1^J	P_2^J	P_3^J	P_1^J	P_2^J	P_3^J
1	0	1	0	1	0	0
2	0	2	0	2	0	0
2.8222	0	2.8222	0	2.8222	0	0
3	0	3	0	2.9585	0	0.0415
4	0	4	0	3.7254	0	0.2746
5	0	5	0	4.4922	0	0.5078
6	0	6	0	5.2590	0	0.741
7	0	7	0	6.0258	0	0.9742
8	0	8	0	6.7926	0	1.2074
9	0	9	0	7.5594	0	1.4406
10	0	10	0	8.3263	0	1.6737
11	0	10	1	9.0931	0	1.9069
12	0	10	2	9.8599	0	2.1401
13	0	10	3	10	0.8395	2.1605
14	0	10	4	10	1.8667	2.1333
15	0	10	5	10	2.8939	2.1061

In order to investigate how the network geometry plays a role in the effectiveness of the proposed schemes, the network illustrated in Fig. 9 with four anchor nodes, two target nodes, and two jammer nodes is considered for two cases (Case 1 and Case 2) corresponding to two different positions of the jammer node 2, as shown in the figure. Target nodes 1 and 2,

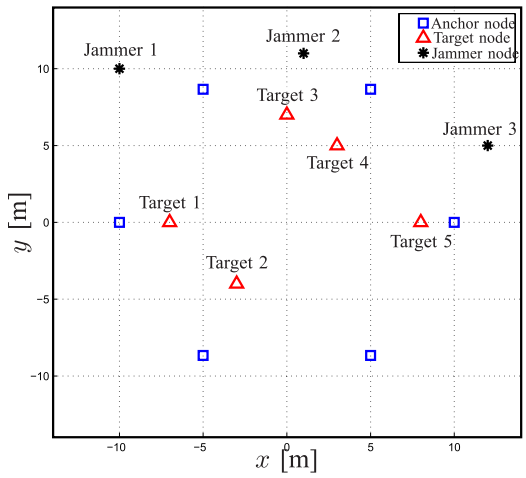

Fig. 7. The network considered in the simulations, where the anchor node positions are $[-10\ 0]$, $[-5\ \ -5\sqrt{3}]$, $[-5\ 5\sqrt{3}]$, $[5\ 5\sqrt{3}]$, $[5\ \ -5\sqrt{3}]$, and $[10\ 0]$ m., the target node positions are $[-7\ 0]$, $[-3\ \ -4]$, $[0\ 7]$, $[3\ 5]$ and $[8\ 0]$ m., and the jammer node positions are $[-10\ 10]$, $[1\ 11]$, and $[12\ 5]$ m.

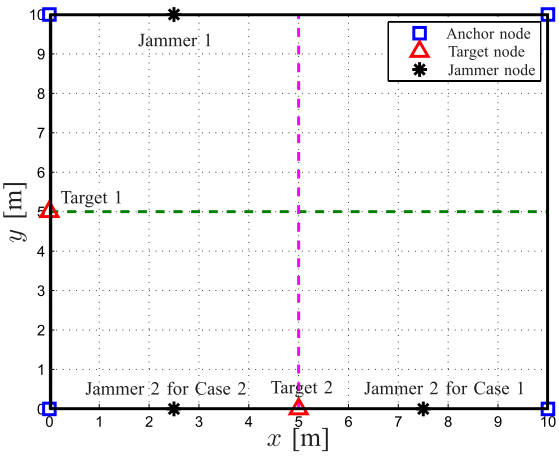

Fig. 9. The network considered in the simulations, where the anchor node positions are $[0\ 0]$, $[10\ 0]$, $[0\ 10]$, and $[10\ 10]$ m., the initial positions of the target nodes are $[0\ 5]$ and $[5\ 0]$ m., the position of jammer node 1 is $[2.5\ 10]$ m., and the position of jammer node 2 is $[7.5\ 0]$ m. (for Case 1) and $[2.5\ 0]$ m (for Case 2).

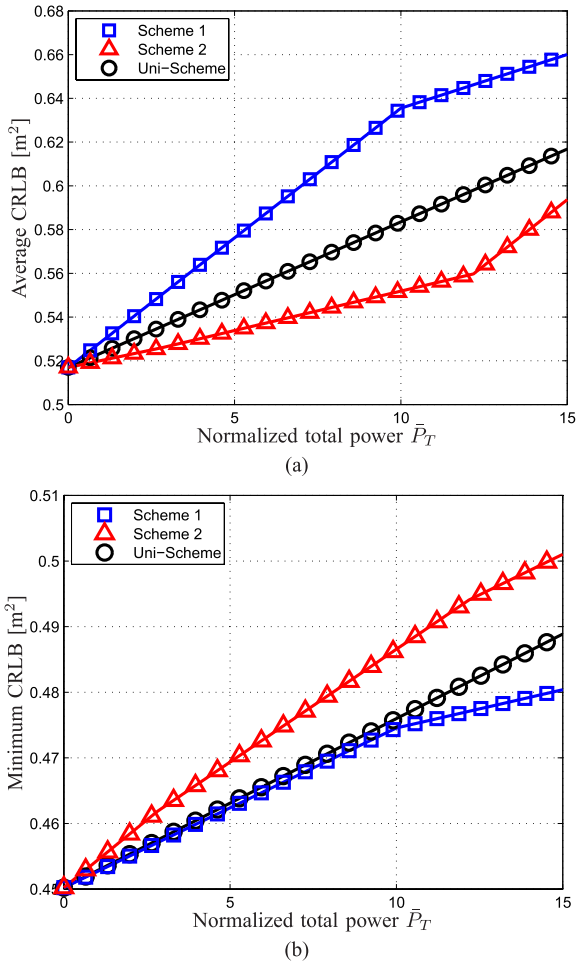

Fig. 8. Comparison of different schemes for power allocation in terms of (a) average CRLB, (b) minimum CRLB for the scenario in Fig. 7.

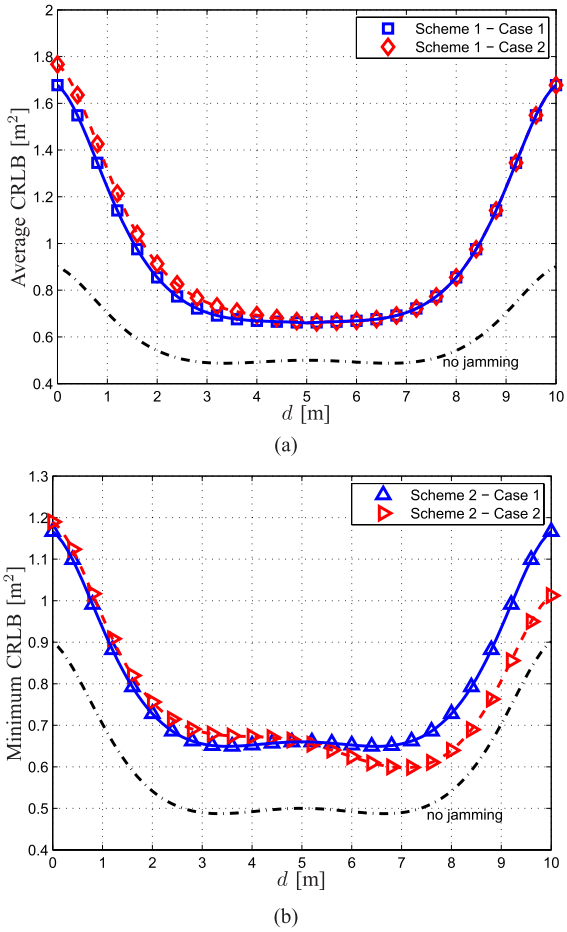

Fig. 10. Comparisons of the optimal jamming schemes in terms of (a) the average CRLB, and (b) the minimum CRLB for Case 1 and Case 2 in Fig. 9. The scenario with no jamming is also illustrated.

initially positioned at $[0\ 5]$ and $[5\ 0]$ m., move simultaneously at the same speed along the green and pink lines, respectively, and the distance from their initial positions is denoted by d. (For example, when $d = 4$ m. the positions of target node 1 and target node 2 are given by $[4\ 5]$ m. and $[5\ 4]$ m., respectively.) The average CRLBs and the minimum CRLBs of the

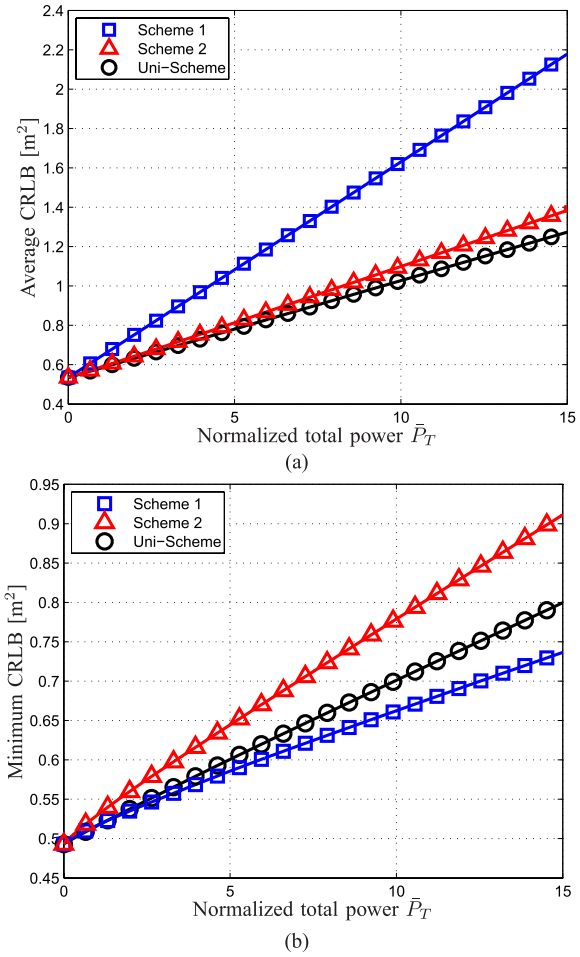

Fig. 11. Comparison of different schemes for power allocation in terms of (a) average CRLB, (b) minimum CRLB, where CRLBs are averaged over the locations of the target nodes, which are uniformly distributed over $[1, 9]$ m. $\times$ $[1, 9]$ m. in Fig. 1.

target nodes corresponding to the optimal schemes (Scheme 1 and Scheme 2) are plotted in Fig. 10 with respect to d, where $\bar{P}_T = 10$ and $P_1^{\text{peak}} = P_2^{\text{peak}} = 20$. In order to provide intuitive explanations, the CRLBs of the target nodes *in the absence of jammer nodes* are plotted in Fig. 10, as well.[10] It is observed from Fig. 10 that the average and minimum CRLBs increase in general for both cases as the target nodes get close to the boundary of the convex hull formed by the anchor nodes. This is expected since the network geometry imposes an increase in the CRLBs as the received powers from two of the anchor nodes decrease significantly when a target node approaches the boundary, which is in accordance with the "no jamming" curves in the figure. Based on a similar reasoning, the average and minimum CRLBs reduce significantly when the target nodes are around the middle of the convex hull formed by the anchor nodes (i.e., at similar distances to all the anchor nodes). In addition, Fig. 10 illustrates that, in Case 1, the jamming performances are symmetric with respect to the center of the square formed by the anchor nodes (i.e., $d = 5$ m.) for both Scheme 1 and Scheme 2, which is due to the fact that the distances of the jammer nodes to target node 1 (and to target node 2) are symmetric around $d = 5$ m. On the other hand, in Case 2, jamming performance is not symmetric around $d = 5$ m. and lower CRLBs are observed for $d > 5$ m. (i.e., reduced jamming performance) since both jammer nodes are far away from target node 1 as d approaches 10 m.

In Fig. 10-(a), which illustrates the average CRLBs for Scheme 1, the jamming performance in Case 2 is better up to $d = 5$ m. and is equal to that of Case 1 after that point, which can be explained based on the geometry of the target and jammer nodes as follows: Scheme 1 aims to assign the whole power to the jammer node which can cause the highest increase in the total CRLBs of the target nodes; hence, it assigns the whole power to the jammer node that has the minimum distance to (one of) the target nodes in this scenario. Therefore, in both cases, the whole power is assigned to jammer node 2 until $d = 5$ m. and to jammer node 1 after that point. Hence, for $d \geq 5$ m., Scheme 1 employs the same strategy of using jammer node 1 only in both cases, which leads to the same jamming performance. For $d < 5$ m., Scheme 1 transmits the whole power from jammer node 2, which has the same distances to target node 2 in both cases but is closer to target node 1 in Case 2, resulting in higher average CRLBs for that case. Based on similar geometric arguments, the differences between Case 1 and Case 2 in Fig. 10-(b) can also be explained. For example, when $d > 5$ m., both jammer node 1 and jammer node 2 are away from target node 1 in Case 2, which leads to reduced jamming performance compared to that in Case 1. Considering the average jamming performances in Case 1 and Case 2, it can be concluded from Fig. 10 that Scheme 1 performs better in Case 2 while Scheme 2 achieves a higher average jamming performance in Case 1. Therefore, it can be concluded for this scenario that the effectiveness of Scheme 2 increases when the jammer nodes are symmetrically positioned with respect to the network geometry (due to the max-min nature of the problem formulation in Scheme 2) but such a symmetry can reduce the efficacy of Scheme 1 in some situations.

To evaluate the average performance of the proposed schemes over different locations for the target nodes, the scenario in Fig. 1 is considered with uniform locations for the target nodes while the jammer and anchor nodes are at fixed locations shown in the figure. In particular, the locations of the target nodes are modeled as independent and identically distributed uniform random variables over $[1, 9]$ m. $\times$ $[1, 9]$ m. In Fig. 11, the average and the minimum CRLBs are plotted versus the normalized total power for different schemes, where the CRLBs are averaged over the locations of the target nodes. It is observed that the performance gap between Scheme 1 and Scheme 2 increases with the normalized total power in this scenario.

Finally, the scenario in Fig. 1 is considered with some uncertainty about the localization related parameters in order to investigate the performance of the proposed schemes in the presence of uncertainty. Referring to Section IV, the uncertainty set $\mathcal{R}_i$ is defined as a linear set specified by $\mathcal{R}_i = [0.75\hat{r}_i, 1.25\hat{r}_i]$, where $\hat{r}_i$ denotes the estimated value

[10] In the absence of jamming, the CRLBs for target nodes 1 and 2 are the same for each value of d.

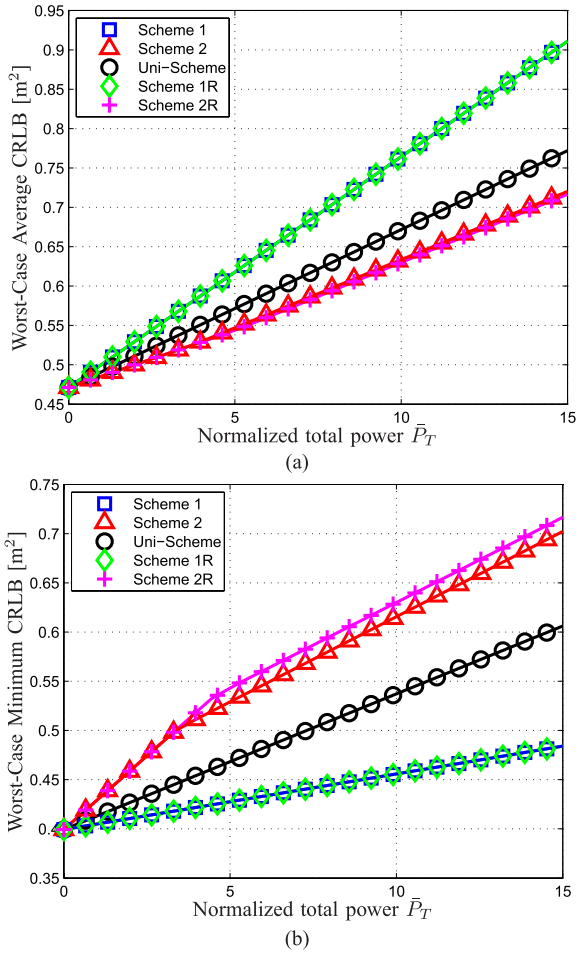

Fig. 12. Comparison of different schemes for power allocation in terms of (a) worst-case average CRLB, (b) worst-case minimum CRLB for the scenario in Fig. 1 with uncertainty.

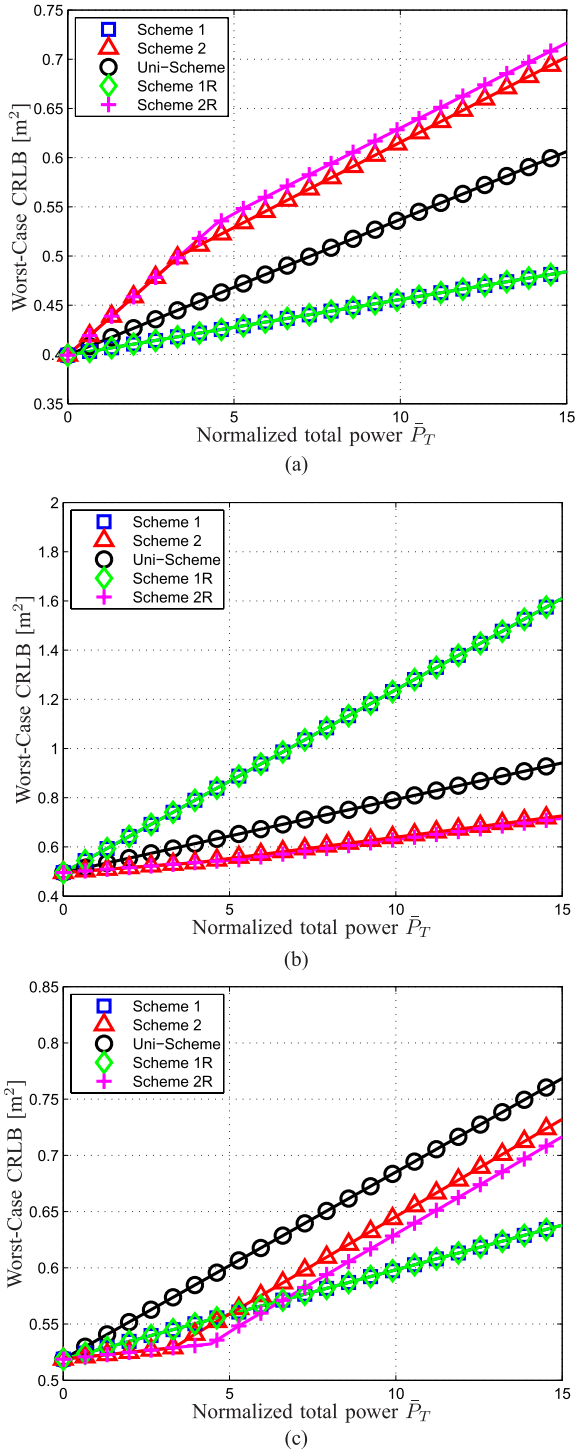

Fig. 13. The worst-case CRLBs for different schemes of power allocation for (a) Target 1, (b) Target 2, and (c) Target 3 (for the scenario in Fig. 1 with uncertainty).

of r_i, which is defined in (15); hence, the true value of r_i is assumed to be within twenty-five percent of the estimated value. Similarly, the linear uncertainty set $\mathcal{C}_i$ defined in (32) is specified by $|\gamma_{i\ell}|^2_{\min} = 0.75|\hat{\gamma}_{i\ell}|^2$ and $|\gamma_{i\ell}|^2_{\max} = 1.25|\hat{\gamma}_{i\ell}|^2$, where $|\hat{\gamma}_{i\ell}|$ represents the estimated value of $|\gamma_{i\ell}|$. In Fig. 12, the 'worst-case' average and minimum CRLBs are plotted versus the normalized total power $\bar{P}_T$ for Scheme 1R, Scheme 2R, Scheme 1, Scheme 2, and Uni-Scheme, where the term 'worst-case' refers to scenarios in which the minimum CRLBs are achieved over the uncertainty set. (Hence, it is the worst-case from the perspective of the jammer nodes.) In addition, Fig. 13 presents the individual worst-case CRLBs versus $\bar{P}_T$, and Table IV illustrates the optimal power allocation policies corresponding to Scheme 1R and Scheme 2R for various values of $\bar{P}_T$. It should be emphasized that Scheme 1 and Scheme 2 are designed according to the estimated parameter values in this scenario whereas Scheme 1R and Scheme 2R are based on the robust design approach described in Section IV. From Fig. 12, Fig. 13, and Table IV, it is observed that Scheme 1R and Scheme 1 have the same performance since the uncertainty does not change the optimal strategy in this scenario (cf. Table I and Remark 5). On the other hand, as noted from Fig. 12-(b), the performance of Scheme 2 is degraded by the uncertainty, especially for large $\bar{P}_T$. However, for small values of $\bar{P}_T$, Scheme 2R and Scheme 2 have the same performance, as stated in Remark 5. To provide insight about this observation, Table I and Table IV can be investigated, which indicate that Scheme 2R and Scheme 2 are equivalent to each other up to $\bar{P}_T = 3.3314$. After this value, the strategies become different and Scheme 2R outperforms

TABLE IV
ALLOCATED POWERS TO JAMMER NODES FOR SCHEMES 1R AND 2R FOR THE SCENARIO IN FIG. 12

$\bar{P}_T$	Scheme 1R			Scheme 2R		
	P_1^J	P_2^J	P_3^J	P_1^J	P_2^J	P_3^J
1	0	0	1	1	0	0
2	0	0	2	2	0	0
3	0	0	3	3	0	0
4	0	0	4	4	0	0
4.4419	0	0	4.4419	4.4419	0	0
5	0	0	5	4.7500	0.2500	0
6	0	0	6	5.2458	0.6449	0.1092
7	0	0	7	5.7241	1.0232	0.2526
8	0	0	8	6.2024	1.4015	0.3961
9	0	0	9	6.6807	1.7798	0.5395
10	0	0	10	7.1590	2.1581	0.6829
11	0	0	11	7.6373	2.5364	0.8263
12	0	0	12	8.1156	2.9147	0.9697
13	0	0	13	8.5939	3.2930	1.1132
14	0	0	14	9.0722	3.6712	1.2566
15	0	0	15	9.5505	4.0495	1.4000

Scheme 2 in terms of the worst-case CRLB. Finally, it is noted from Fig. 13 that the performance gap between Scheme 2R and Scheme 2 is mainly due to the differences between the achieved worst-case CRLBs for target node 1 and target node 3.

VI. EXTENSIONS AND FUTURE WORK

Since the network geometry has important effects on the performance of jamming (see Remark 3 and Fig. 10), the locations of the jammer nodes can also be considered as additional optimization variables for a more generic formulation. In that case, the following problem can be obtained for the average CRLB criterion (cf. (17)):

$$\begin{aligned} \underset{\boldsymbol{p}^J,\{z_\ell\}_{\ell=1}^{N_J}}{\text{maximize}} \ & \left(\sum_{i=1}^{N_T} r_i\, \boldsymbol{a}_i^T\right)\boldsymbol{p}^J \\ \text{subject to } & \mathbf{1}^T\boldsymbol{p}^J \le P_T \\ & 0 \le P_\ell^J \le P_\ell^{\text{peak}}, \quad \ell = 1,2,\ldots,N_J \\ & z_\ell \in \mathcal{S}_\ell, \quad \ell = 1,2,\ldots,N_J \end{aligned} \tag{36}$$

where the maximization is over both the powers and the locations of the jammer nodes, denoted by $\boldsymbol{p}^J$ and $\{z_\ell\}_{\ell=1}^{N_J}$, respectively. In addition, $\mathcal{S}_\ell$ represents the feasible locations for the ℓth jammer node in the network. For example, the jammer nodes cannot be located very closely to the target nodes in practice in order not to be detected.

To obtain the solution of (36), a relation should be specified between z_ℓ's and $\boldsymbol{a}_i$'s, where $\boldsymbol{a}_i = [|\gamma_{i1}|^2 \cdots |\gamma_{iN_J}|^2]^T$, as defined in (10). For example, similar to [20] and [21], $|\gamma_{i\ell}|^2$ can be calculated as $|\gamma_{i\ell}|^2 = \kappa_{i\ell}(d_0/\|z_\ell - \boldsymbol{x}_i\|)^\nu$ for $\|z_\ell - \boldsymbol{x}_i\| > d_0$, where $\boldsymbol{x}_i$ is the location of target node i, ν is the path-loss exponent, $\kappa_{i\ell}$ is a constant (depending on antenna characteristics and average channel attenuation), and d_0 is the reference distance for the antenna far-field.[11] Then, the solution of (36) is specified by the following proposition:

[11]It is assumed that $\|z_\ell - \boldsymbol{x}_i\| > d_0$ holds for all $z_\ell \in \mathcal{S}_\ell$, where $\ell \in \{1,\ldots,N_J\}$.

Proposition 6: Define z_ℓ^* as follows:

$$z_\ell^* = \underset{z_\ell \in \mathcal{S}_\ell}{\arg\max} \sum_{i=1}^{N_T} r_i |\gamma_{i\ell}|^2 \quad \text{for } \ell \in \{1,\ldots,N_J\}. \tag{37}$$

Also, define $\boldsymbol{w}^*$ as the value of $\sum_{i=1}^{N_T} r_i\, \boldsymbol{a}_i$ at $z_1^*,\ldots,z_{N_J}^*$. Then, the optimal solution to (36) is specified by the jammer locations $z_1^*,\ldots,z_{N_J}^*$ and the corresponding power levels

$$\boldsymbol{p}_{\text{opt}}^J(h^*(j)) = \min\left\{ P_T - \sum_{l=1}^{j-1} \boldsymbol{p}_{\text{opt}}^J(h^*(l)),\, P_{h^*(j)}^{\text{peak}} \right\} \tag{38}$$

for $j = 1,\ldots,N_J$, where $h^*(j)$ represents the index of the jth largest element of $\boldsymbol{w}^*$, and $\boldsymbol{p}_{\text{opt}}^J(h^*(j))$ denotes the $h^*(j)$th element of $\boldsymbol{p}_{\text{opt}}^J$.

Proof: Define $\boldsymbol{w}$ as $\boldsymbol{w} \triangleq \sum_{i=1}^{N_T} r_i\, \boldsymbol{a}_i$ and express the objective function in (36) as $\boldsymbol{w}^T\boldsymbol{p}^J$. It is noted that the jammer locations $z_1,\ldots,z_{N_J}$ only affect the $\boldsymbol{w}$ term in the objective function. In addition, from (10), it is observed that the ℓth element of $\boldsymbol{w}$ depends on the location of jammer node ℓ only. Since the power terms are always non-negative, the solution of (36) requires the maximization of $\boldsymbol{w}$ over $z_1,\ldots,z_{N_J}$ subject to $z_\ell \in \mathcal{S}_\ell$ for $\ell = 1,2,\ldots,N_J$, which can be decomposed into the following N_J problems:

$$\max_{z_\ell \in \mathcal{S}_\ell} \sum_{i=1}^{N_T} r_i |\gamma_{i\ell}|^2, \ \ell = 1,2,\ldots,N_J \tag{39}$$

where $\sum_{i=1}^{N_T} r_i |\gamma_{i\ell}|^2$ corresponds to the ℓth element of $\boldsymbol{w}$. Hence, the optimal locations of the jammer nodes are obtained as in (37). After obtaining the optimal locations of the jammer nodes, the optimization problem in (36) reduces to a problem which is in the same form as that in (17). Hence, the result in Proposition 2 can be employed to obtain the optimal power allocation strategy in (38) (cf. (18)). ■

Proposition 6 implies that the optimal location for each jammer node is related to the CRLBs of the target nodes in the absence of jamming (since $r_i N_0/2$ corresponds to the CRLB of target node i in the absence of jamming) and the channel gains between the jammer node and the target nodes. Once the optimal locations of the jammer nodes are determined based on (37), the optimal power allocation strategy can be obtained via (38), which is similar to Scheme 1 in Section III. In a similar fashion, the robust power allocation algorithm in Section IV, Scheme 1-R, can also be extended to the case of joint optimization of the powers and the locations of the jammer nodes.

Remark 6: For identical jammer nodes and for the same feasible region for each jammer node (i.e., $\mathcal{S}_\ell = \mathcal{S}$, $\forall \ell \in \{1,\ldots,N_J\}$), it can be concluded from (37) that the optimal locations for the jammer nodes are the same; that is, $z_\ell^* = z^*$, $\forall \ell \in \{1,\ldots,N_J\}$. In this case, a jammer node or multiple jammer nodes located at z^* and transmitting a (total) power of P_T yields the solution of (36).

For the minimum CRLB criterion, the following problem can be considered for the joint optimization of the powers

and the locations of the jammer nodes (cf. (19)):

$$\begin{aligned} \underset{\boldsymbol{p}^J,\{z_\ell\}_{\ell=1}^{N_J}}{\text{maximize}} \quad & \min_{i\in\{1,\ldots,N_T\}} r_i \boldsymbol{a}_i^T \boldsymbol{p}^J + r_i N_0/2 \\ \text{subject to} \quad & \mathbf{1}^T \boldsymbol{p}^J \le P_T \\ & 0 \le P_\ell^J \le P_\ell^{\text{peak}}, \quad \ell = 1, 2, \ldots, N_J \\ & \boldsymbol{z}_\ell \in \mathcal{S}_\ell, \quad \ell = 1, 2, \ldots, N_J \end{aligned} \tag{40}$$

In this scenario, it is challenging to obtain a simple expression for the optimal locations of the jammer nodes and the corresponding optimal power levels. The theoretical and algorithmic investigations of the problem in (40) and its robust versions are considered as an important direction for future work.

In the previous sections, jammer nodes are modeled to transmit *Gaussian noise* to degrade the performance of a wireless localization system. This is a common model for jamming in the literature (e.g., [45]–[47]), which can be motivated as follows: When the ranging signals between the anchor and target nodes are unknown to the jammer nodes, the jammer nodes can constantly transmit *noise* to reduce the performance of range estimation (hence, localization). Since the Gaussian distribution corresponds to the worst-case scenario among all possible noise distributions,[12] the jammer nodes that transmit Gaussian noise are employed for efficient jamming [45]–[47]. In practice, the ranging signals between the anchor and target nodes can be unknown to the jammer nodes in certain scenarios such as military applications and private ranging [4], [51].

If the ranging signals between the anchor and target nodes are known to the jammer nodes (which can be possible, e.g., when some standard signals are employed for ranging), the jammer nodes can severely degrade ranging and localization performance. In particular, each jammer node can transmit, according to a certain strategy, the same ranging signal as that employed by an anchor node, and the target node, the aim of which is to estimate the time-of-arrival (TOA) of the first incoming ranging signal component, can sometimes erroneously perform its estimation based on a signal sent by a jammer node instead of that from the anchor node. In this case, the exact values for the powers of the jammer nodes are not critical as long as the ranging signals from the jammer nodes arrive at the target node with sufficiently high power levels (assuming that signal components above a certain threshold are employed for TOA estimation as in [52]). Hence, the optimal power allocation problem studied in Section III is not relevant in such cases. To present a formulation of the theoretical limits in this scenario, the received signal related to target node i and anchor node j can be expressed as follows (cf. (1)):

$$\begin{aligned} \tilde{r}_{ij}(t) = & \sum_{k=1}^{L_{ij}} \alpha_{ij}^k s(t-\tau_{ij}^k) + \sum_{\ell=1}^{N_J}\sum_{k=1}^{\tilde{L}_{i\ell}} \tilde{\alpha}_{i\ell}^k s(t-\tilde{\tau}_{i\ell}^k - T_\ell) \\ & + n_{ij}(t) \end{aligned} \tag{41}$$

[12]For example, for a Gaussian channel and a Gaussian input signal, the worst-case form of the jamming signal is also Gaussian in terms of minimizing the mutual information between the input and the output [48], [49]. Also, for an additive noise channel with a Gaussian input, the worst-case noise distribution (for a given mean and variance) that maximizes the MSE of estimating the input given the channel output corresponds to Gaussian distribution, which can be proved based on the linearity of optimal estimation in the presence of Gaussian noise [50].

for $t \in [0, T_{\text{obs}}]$, where the first and the third terms are as in (1), and the second term represents the signals from the jammer nodes arriving at target node i, with $\tilde{\alpha}_{i\ell}^k$ and $\tilde{\tau}_{i\ell}^k$ denoting, respectively, the amplitude and delay of the kth multipath component between jammer node ℓ and target node i, and $\tilde{L}_{i\ell}$ being the number of paths between target node i and jammer node ℓ. Also, T_ℓ represents the relative delay of the ranging signal sent by jammer node ℓ with respect to that sent by anchor node j. (In fact, each jammer node can also transmit multiple copies of the ranging signal, which can easily be incorporated into the second term in (41), but this is omitted for simplicity by assuming that one ranging signal from each jammer node is present in the observation interval $t \in [0, T_{\text{obs}}]$.)

The received signal $\tilde{r}_{ij}(t)$ in (41) should be used to extract information about the distance (range) between target node i and anchor node j. From the expression in (41), it is observed that when the jammer nodes transmit the same signals as the anchor node, the total jamming signal (the second term in (41)) becomes similar to multipath interference. In this case, if the first signal path arriving at the target node is originated from the anchor node; that is, if $T_\ell > 0$, $\forall \ell$, and if no signal components due to the jammer nodes overlap with that first signal component, then it can be shown, based on similar arguments to those in [53], that the jammer nodes do not affect (reduce) the amount of information obtained from $\tilde{r}_{ij}(t)$; i.e., $\tilde{r}_{ij}(t)$ contributes to the CRLB for the localization of target node i as if no jamming were present. However, it is commonly possible for the jammer nodes to develop transmission strategies (e.g., by sending a sufficiently large number of ranging signals in each observation interval) to make sure that the first signal component arriving at the target node is due to one of the jammer nodes (that is, there exist $\ell \in \{1, \ldots, N_J\}$ such that $T_\ell < 0$ in (41)). In this scenario, the analysis in [54] can be invoked to show that in the absence of prior information about the statistics of the minimum T_ℓ (i.e., the minimum of T_ℓ over $\ell \in \{1, \ldots, N_J\}$), the received signal $\tilde{r}_{ij}(t)$ in (41)) does not contribute to the accuracy of localization; that is, the CRLB for target node i cannot utilize $\tilde{r}_{ij}(t)$ as it does not carry any useful information. In this manner, the jammer nodes can reduce the number of anchor nodes that can effectively be used in the localization of the target nodes. Hence, when the jammer nodes know the ranging signals employed for localization and employ an effective strategy to send the same ranging signals as the anchor nodes, it becomes possible to disable the wireless localization system (i.e., to cause unacceptably high localization errors) unless the anchor and target nodes do not take any preventive actions. To mitigate the effects of jamming in such cases, the target nodes can try to detect the presence of jammer nodes by examining the structural differences in the received signals due to the signals from the jammer nodes and to employ different ranging signals in each cycle so that the jammer nodes cannot know the signal structures in advance.

VII. Concluding Remarks

In this study, jamming of wireless localization systems has been investigated. Considering the CRLB on location

estimation accuracy, two different schemes have been proposed to maximize certain functions of the CRLBs of the target nodes. In the first approach, power levels have been allocated to jammer nodes in order to maximize the average CRLB of the target nodes whereas in the second approach the power allocation to jammer nodes has been performed for the aim of maximizing the minimum CRLB of the target nodes. Both techniques have been formulated as linear programs, and a closed-form expression has been obtained for the average CRLB maximization problem. In addition, the full total power utilization property has been presented for the minimum CRLB maximization problem, and its closed-form solution has been obtained under certain conditions when the total power is smaller than a specific threshold. Furthermore, in the absence of peak power constraints, it has been proved that an optimal strategy to maximize the minimum CRLB can be obtained by allocating non-zero power to at most N_T jammer nodes, where N_T is the number of target nodes. In the presence of parameter uncertainty, the robust versions of the power allocation schemes have been proposed, and it has been shown that the theoretical results are valid for this scenario, as well. Simulation results have shown the promising performance of the proposed schemes with respect to the uniform power allocation scheme.

REFERENCES

[1] S. Gezici, M. R. Gholami, S. Bayram, and M. Jansson, "Optimal jamming of wireless localization systems," in *Proc. IEEE Int. Conf. Commun. Workshops (ICCW)*, Jun. 2015, pp. 877–882.

[2] R. Zekavat and R. M. Buehrer, *Handbook of Position Location: Theory, Practice and Advances*. New York, NY, USA: Wiley, 2011.

[3] J. Figueiras and S. Frattasi, *Mobile Positioning and Tracking: From Conventional to Cooperative Techniques*. West Sussex, U.K.: Wiley, 2010.

[4] Z. Sahinoglu, S. Gezici, and I. Güvenc, *Ultra-Wideband Positioning Systems: Theoretical Limits, Ranging Algorithms, and Protocols*. New York, NY, USA: Cambridge Univ. Press, 2008.

[5] S. Gezici, "A survey on wireless position estimation," *Wireless Pers. Commun.*, vol. 44, no. 3, pp. 263–282, Feb. 2008.

[6] Y. Shen and M. Z. Win, "Fundamental limits of wideband localization—Part I: A general framework," *IEEE Trans. Inf. Theory*, vol. 56, no. 10, pp. 4956–4980, Oct. 2010.

[7] G. Zanca, F. Zorzi, A. Zanella, and M. Zorzi, "Experimental comparison of RSSI-based localization algorithms for indoor wireless sensor networks," in *Proc. Workshop Real-World Wireless Sensor Netw. (REALWSN)*, Glasgow, U.K., Apr. 2008, pp. 1–5.

[8] H. Hu and N. Wei, "A study of GPS jamming and anti-jamming," in *Proc. 2nd Int. Conf. Power Electron. Intell. Transp. Syst. (PEITS)*, vol. 1. Dec. 2009, pp. 388–391.

[9] D. Lu, R. Wu, and H. Liu, "Global positioning system anti-jamming algorithm based on period repetitive CLEAN," *IET Radar, Sonar Navigat.*, vol. 7, no. 2, pp. 164–169, Feb. 2013.

[10] Y. D. Zhang and M. G. Amin, "Anti-jamming GPS receiver with reduced phase distortions," *IEEE Signal Process. Lett.*, vol. 19, no. 10, pp. 635–638, Oct. 2012.

[11] Y. Shen and M. Z. Win, "Energy efficient location-aware networks," in *Proc. IEEE Int. Conf. Commun. (ICC)*, May 2008, pp. 2995–3001.

[12] W. W.-L. Li, Y. Shen, Y. J. Zhang, and M. Z. Win, "Efficient anchor power allocation for location-aware networks," in *Proc. IEEE Int. Conf. Commun. (ICC)*, Jun. 2011, pp. 1–6.

[13] W. W.-L. Li, Y. Shen, Y. J. Zhang, and M. Z. Win, "Robust power allocation via semidefinite programming for wireless localization," in *Proc. IEEE Int. Conf. Commun. (ICC)*, Jun. 2012, pp. 3595–3599.

[14] W. W.-L. Li, Y. Shen, Y. J. Zhang, and M. Z. Win, "Robust power allocation for energy-efficient location-aware networks," *IEEE/ACM Trans. Netw.*, vol. 21, no. 6, pp. 1918–1930, Dec. 2013.

[15] T. Wang, G. Leus, and L. Huang, "Ranging energy optimization for robust sensor positioning based on semidefinite programming," *IEEE Trans. Signal Process.*, vol. 57, no. 12, pp. 4777–4787, Dec. 2009.

[16] T. Wang and G. Leus, "Ranging energy optimization for robust sensor positioning with collaborative anchors," in *Proc. IEEE Int. Conf. Acoust. Speech Signal Process. (ICASSP)*, Mar. 2010, pp. 2714–2717.

[17] H. Godrich, A. P. Petropulu, and H. V. Poor, "Power allocation strategies for target localization in distributed multiple-radar architectures," *IEEE Trans. Signal Process.*, vol. 59, no. 7, pp. 3226–3240, Jul. 2011.

[18] S. Bayram, N. D. Vanli, B. Dulek, I. Sezer, and S. Gezici, "Optimum power allocation for average power constrained jammers in the presence of non-Gaussian noise," *IEEE Commun. Lett.*, vol. 16, no. 8, pp. 1153–1156, Aug. 2012.

[19] Y. Shen, W. Dai, and M. Z. Win, "Optimal power allocation for active and passive localization," in *Proc. IEEE Global Commun. Conf. (GLOBECOM)*, Dec. 2012, pp. 3713–3718.

[20] Y. Shen, W. Dai, and M. Z. Win, "Power optimization for network localization," *IEEE/ACM Trans. Netw.*, vol. 22, no. 4, pp. 1337–1350, Aug. 2014.

[21] T. Zhang, A. Molisch, Y. Shen, Q. Zhang, and M. Z. Win, "Joint power and bandwidth allocation in cooperative wireless localization networks," in *Proc. IEEE Conf. Commun. (ICC)*, Jun. 2014, pp. 2611–2616.

[22] W. Li, T. Zhang, Y. Shen, A. F. Molisch, and Q. Zhang, "Robust resource allocation in wireless localization networks," in *Proc. IEEE/CIC Int. Conf. Commun. China (ICCC)*, Oct. 2014, pp. 442–447.

[23] T. Cheng, P. Li, and S. Zhu, "An algorithm for jammer localization in wireless sensor networks," in *Proc. IEEE 26th Int. Conf. Adv. Inf. Netw. Appl. (AINA)*, Mar. 2012, pp. 724–731.

[24] T. Cheng, P. Li, and S. Zhu, "Multi-jammer localization in wireless sensor networks," in *Proc. 7th Int. Conf. Comput. Intell. Secur. (CIS)*, Dec. 2011, pp. 736–740.

[25] Y. Liu and W. Trappe, "Jammer forensics: Localization in peer to peer networks based on Q-learning," in *Proc. IEEE Int. Conf. Acoust. Speech Signal Process. (ICASSP)*, Apr. 2015, pp. 1737–1741.

[26] H. Liu, W. Xu, Y. Chen, and Z. Liu, "Localizing jammers in wireless networks," in *Proc. IEEE Int. Conf. Pervasive Comput. Commun. (PerCom)*, Mar. 2009, pp. 1–6.

[27] S. Gezici, S. Bayram, M. R. Gholami, and M. Jansson, "Optimal jammer placement in wireless localization networks," in *Proc. IEEE Int. Workshop Signal Process. Adv. Wireless Commun. (SPAWC)*, Jun./Jul. 2015, pp. 665–669.

[28] M. K. Simon, J. K. Omura, R. A. Scholtz, and B. K. Levitt, *Spread Spectrum Communications*, vol. 1. Rockville, MD, USA: Computer Science Press, 1985.

[29] M. Weiss and S. C. Schwartz, "On optimal minimax jamming and detection of radar signals," *IEEE Trans. Aerosp. Electron. Syst.*, vol. AES-21, no. 3, pp. 385–393, May 1985.

[30] R. J. McEliece and W. E. Stark, "An information theoretic study of communication in the presence of jamming," in *Proc. Int. Conf. Commun. (ICC)*, vol. 3. 1981, pp. 45.3.1–45.3.5.

[31] W. Xu, W. Trappe, Y. Zhang, and T. Wood, "The feasibility of launching and detecting jamming attacks in wireless networks," in *Proc. Annu. Int. Conf. Mobile Comput. Netw. (MobiCom)*, 2005, pp. 46–57.

[32] W. Xu, K. Ma, W. Trappe, and Y. Zhang, "Jamming sensor networks: Attack and defense strategies," *IEEE Netw.*, vol. 20, no. 3, pp. 41–47, May 2006.

[33] Y. Qi, H. Suda, and H. Kobayashi, "On time-of-arrival positioning in a multipath environment," in *Proc. IEEE 60th Veh. Technol. Conf. (VTC-Fall)*, vol. 5. Sep. 2004, pp. 3540–3544.

[34] S. Gezici *et al.*, "Localization via ultra-wideband radios: A look at positioning aspects for future sensor networks," *IEEE Signal Process. Mag.*, vol. 22, no. 4, pp. 70–84, Jul. 2005.

[35] Y. Qi, H. Kobayashi, and H. Suda, "Analysis of wireless geolocation in a non-line-of-sight environment," *IEEE Trans. Wireless Commun.*, vol. 5, no. 3, pp. 672–681, Mar. 2006.

[36] A. Mallat, S. Gezici, D. Dardari, C. Craeye, and L. Vandendorpe, "Statistics of the MLE and approximate upper and lower bounds—Part I: Application to TOA estimation," *IEEE Trans. Signal Process.*, vol. 62, no. 21, pp. 5663–5676, Nov. 2014.

[37] D. Dardari and M. Z. Win, "Ziv–Zakai bound on time-of-arrival estimation with statistical channel knowledge at the receiver," in *Proc. IEEE Int. Conf. Ultra-Wideband (ICUWB)*, Sep. 2009, pp. 624–629.

[38] S. Boyd and L. Vandenberghe, *Convex Optimization*. Cambridge, U.K.: Cambridge Univ. Press, 2004.

[39] Y. Karisan, D. Dardari, S. Gezici, A. D'Amico, and U. Mengali, "Range estimation in multicarrier systems in the presence of interference: Performance limits and optimal signal design," *IEEE Trans. Wireless Commun.*, vol. 10, no. 10, pp. 3321–3331, Oct. 2011.
[40] A. Goldsmith, *Wireless Communications*. Cambridge, U.K.: Cambridge Univ. Press, 2005.
[41] M. A. Khojastepour and B. Aazhang, "The capacity of average and peak power constrained fading channels with channel side information," in *Proc. IEEE Wireless Commun. Netw. Conf. (WCNC)*, vol. 1. Mar. 2004, pp. 77–82.
[42] R. T. Rockafellar, *Convex Analysis*. Princeton, NJ, USA: Princeton Univ. Press, 1968.
[43] W. Dai, Y. Shen, and M. Z. Win, "Sparsity-inspired power allocation for network localization," in *Proc. IEEE Int. Conf. Commun. (ICC)*, Jun. 2013, pp. 2785–2790.
[44] C. Qin, L. Song, T. Zhang, Y. Shen, A. Molisch, and Q. Zhang, "Joint power and spectrum optimization in wireless localization networks," in *Proc. IEEE Int. Conf. Commun. Workshop (ICCW)*, Jun. 2015, pp. 859–864.
[45] J. Gao, S. A. Vorobyov, H. Jiang, and H. V. Poor, "Worst-case jamming on MIMO Gaussian channels," *IEEE Trans. Signal Process.*, vol. 63, no. 21, pp. 5821–5836, Nov. 2015.
[46] E. A. Jorswieck, H. Boche, and M. Weckerle, "Optimal transmitter and jamming strategies in Gaussian MIMO channels," in *Proc. IEEE 61st Veh. Technol. Conf. (VTC-Spring)*, vol. 2. May/Jun. 2005, pp. 978–982.
[47] G. T. Amariucai, S. Wei, and R. Kannan, "Gaussian jamming in block-fading channels under long term power constraints," in *Proc. IEEE Int. Symp. Inf. Theory (ISIT)*, Jun. 2007, pp. 1001–1005.
[48] S. N. Diggavi and T. M. Cover, "The worst additive noise under a covariance constraint," *IEEE Trans. Inf. Theory*, vol. 47, no. 7, pp. 3072–3081, Nov. 2001.
[49] R. Bustin, H. V. Poor, and S. Shamai (Shitz), "Worst additive noise: An information-estimation view," in *Proc. IEEE 28th Conv. Elect. Electron. Eng. Israel*, Dec. 2014, pp. 1–4.
[50] S. Kay, *Fundamentals of Statistical Signal Processing: Estimation Theory*. Englewood Cliffs, NJ, USA: Prentice-Hall, 1993.
[51] Z. Sahinoglu and S. Gezici, "Ranging in the IEEE 802.15.4a standard," in *Proc. IEEE Wireless Microw. Technol. Conf. (WAMICON)*, Clearwater, FL, USA, Dec. 2006, pp. 1–5.
[52] I. Guvenc and Z. Sahinoglu, "Threshold-based TOA estimation for impulse radio UWB systems," in *Proc. IEEE Int. Conf. UWB (ICU)*, Sep. 2005, pp. 420–425.
[53] S. Gezici, "Theoretical limits for estimation of periodic movements in pulse-based UWB systems," *IEEE J. Sel. Topics Signal Process.*, vol. 1, no. 3, pp. 405–417, Oct. 2007.
[54] Y. Qi, H. Kobayashi, and H. Suda, "On time-of-arrival positioning in a multipath environment," *IEEE Trans. Veh. Technol.*, vol. 55, no. 5, pp. 1516–1526, Sep. 2006.

Sinan Gezici (S'03–M'06–SM'11) received the B.S. degree from Bilkent University, Turkey, in 2001, and the Ph.D. degree in electrical engineering from Princeton University, in 2006. From 2006 to 2007, he was with Mitsubishi Electric Research Laboratories, Cambridge, MA. Since 2007, he has been with the Department of Electrical and Electronics Engineering, Bilkent University, where he is currently an Associate Professor.

He has authored the book entitled *Ultrawideband Positioning Systems: Theoretical Limits, Ranging Algorithms, and Protocols* (Cambridge University Press, 2008). His research interests are in the areas of detection and estimation theory, wireless communications, and localization systems. He is an Associate Editor of the IEEE TRANSACTIONS ON COMMUNICATIONS, the IEEE WIRELESS COMMUNICATIONS LETTERS, and the *Journal of Communications and Networks*.

Mohammad Reza Gholami (S'09–M'14) received the Ph.D. degree from Chalmers University of Technology, Gothenburg, Sweden, in 2013. From 2012 to 2013, he was a Visiting Researcher with the Adaptive Systems Laboratory, University of California at Los Angeles. From 2014 to 2015, he was a Post-Doctoral Research Fellow with the Department of Signal Processing, KTH Royal Institute of Technology, Stockholm, Sweden. He is currently a Senior Data Scientist with Campanja AB. His main interests are statistical inference, distributed estimation, wireless network positioning, network wide synchronization, and data analytics.

Suat Bayram (S'09–M'12) received the B.S. degree from Middle East Technical University, Ankara, Turkey, in 2007, and the M.S. and Ph.D. degrees from Bilkent University, Ankara, in 2009 and 2011, respectively. He is currently an Associate Professor with the Department of Electrical and Electronics Engineering, Turgut Ozal University, where he has been a Faculty Member since 2013. His research interests are in the fields of statistical signal processing and communications.

Magnus Jansson received the M.S., Technical Licentiate, and Ph.D. degrees from the KTH Royal Institute of Technology, Stockholm, Sweden, in 1992, 1995, and 1997, respectively, all in electrical engineering. From 1997 to 1998, he was a Lecturer with the Control Department, KTH Royal Institute of Technology. He was with the Department of Electrical and Computer Engineering, University of Minnesota, from 1998 to 1999. He was an Assistant Professor from 1998 to 2003 and an Associate Professor from 2003 to 2012 with the Signal Processing Department, KTH Royal Institute of Technology, where he has been a Professor since 2013. In 2002, he was appointed as a Docent in signal processing with the KTH Royal Institute of Technology.

His research interests include statistical signal processing, navigation and positioning, sensor array processing, time series analysis, and system identification. He served as an Associate Editor of the IEEE SIGNAL PROCESSING LETTERS from 2008 to 2012, and a Senior Area Editor of the IEEE SIGNAL PROCESSING LETTERS (2012–2014). He has been an Associate Editor of the *EURASIP Journal on Advances in Signal Processing* (2007–), and *EURASIP Signal Processing* (2015–).